NASA CR-132377

# STUDY TO DETERMINE AND ANALYZE THE STRENGTH OF HIGH MODULUS GLASS IN EPOXY-MATRIX COMPOSITES

by

J. F. BACON

FINAL REPORT

JANUARY 1974

Prepared for

NASA-Langley Research Center
Contract NAS1—11648

United Aircraft
Research Laboratories

UNITED AIRCRAFT CORPORATION

EAST HARTFORD, CONNECTICUT 06108

United Aircraft Research Laboratories

UNITED AIRCRAFT CORPORATION

EAST HARTFORD, CONNECTICUT

Report N911396-13

# Study to Determine and Analyze the Strength of High Modulus Glass in Epoxy-Matrix Composites

Final Report

Contract NAS1-11648

REPORTED BY _____
J. F. Bacon

APPROVED BY _____
M. A. DeCrescente, Chief
High Temperature Materials

DATE January 1974

NO. OF PAGES 51

COPY NO. _____

## ABSTRACT

A short program of glass composition research was conducted in an attempt to produce a high modulus, high strength beryllia-free glass fiber. This program was built on the previous research carried out at UARL in developing high modulus, high strength glass fibers which had a 5 weight percent beryllia content. The fibers resulting from the composition program were then used to produce fiber reinforced-epoxy resin composites which were compared with composites reinforced by commercial high modulus glass fibers, Thornel S graphite fiber, and hybrids where the external quarters were reinforced with Thornel S graphite fiber and the interior half with UARL glass fiber as well as the reverse hybrid. The composites were given tensile strength, compressive strength, short-beam shear strength, creep and fatigue tests. Comments are included on the significance of the test data.

Report N911396-13

Study to Determine and Analyze the Strength of High Modulus Glass in Epoxy-Matrix Composites

TABLE OF CONTENTS

TABLE OF CONTENTS (Cont'd)

# LIST OF TABLES

# LIST OF ILLUSTRATIONS

## SUMMARY

Forty-four new non-beryllia glass compositions were developed during the contractual period. Seven of these compositions proved readily fiberizable. But, the best of the new compositions, UARL 527, had a fiber modulus of 16.6 million psi and a density of 3.31 gms/cm$^3$ compared to a non-beryllia composition originated under earlier contracts, UARL 129, which had a fiber modulus of 16.7 million psi and a density of 3.28 gms/cm$^3$. It was decided, therefore, to use UARL 129 to produce glass fiber-epoxy resin composites for evaluation.

UARL 129 glass fiber with a modulus of 16.7 million psi had a single filament strength ranging from 726,666 psi to 756,756 psi in six consecutive measurements. This same glass when sized with a UARL proprietary size had a retained strength of 563,000 psi or a specific strength 12 percent greater than UARL "S" glass fibers produced from Ferro "S" glass marbles sized with same sizing and used to reinforce the same epoxy resin.

Composites formed from UARL 129 glass fiber and epoxy resin were then compared with four other types of composites, namely, UARL "S" glass fiber-epoxy resin, Thornel 75S graphite fiber-epoxy resin, a hybrid composite with the outer quarters formed from UARL 129 glass fiber epoxy resin and the interior half from Thornel 75S graphite fiber epoxy resin, and finally the reverse hybrid where the outer quarters were formed from Thornel 75S graphite fiber-epoxy resin and the interior half from UARL 129 glass fiber-epoxy resin. In these comparisons the composites with UARL 129 glass fiber and epoxy resin had improved tensile strength and compressive strength when compared to the other composites. The hybrid composite with the UARL 129 glass fiber-epoxy resin composite forming the central composite and the graphite fiber composite on the external quarters had more than twice the compressive strength of either the composite formed solely with Thornel 75S graphite fiber-epoxy resin or the hybrid composite when the graphite fiber was used to reinforce the interior half. In short beam shear tests, again the hybrid composite with UARL 129 glass fiber reinforcing the interior half was markedly superior to both the pure graphite fiber composite and the hybrid composite in which the Thornel 75S graphite fiber composite formed the interior half.

Creep tests of the UARL 129 glass fiber-epoxy resin composites showed no creep but did prove that the UARL 129 glass fiber composite was more resistant to static fatigue than a similar composite formed with "S" glass.

Finally, the contract showed evidence that still higher modulus and strong non-beryllia glass fibers can be achieved readily, that these fibers will be competitive in cost with commercially available high modulus glass fiber, and that these fibers can be drawn at high rates just as are the more usual glass fibers. However, the contract also showed when the short-beam shear data are scrutinized that further work on a sizing for this new non-beryllia glass fiber is necessary to more fully retain the properties of the fiber when added to an epoxy resin.

# INTRODUCTION

Contract NAS1-11648 between NASA-Langley and UARL was a year long contract whose purpose was the removal of the beryllia content of the high modulus glasses previously developed by UARL under the prior NASA contracts NASW-1301, NASW-2013, and NASW-2209, without appreciable degradation of the outstanding properties of the beryllia glasses. The contract essentially called for the development of the non-beryllia glass in the first four months of the contract and the making and testing of numerous glass fiber-epoxy resin composites in the last eight months of the contract in which the newly developed non-beryllia glass would form the reinforcing agent. A small amount of the research effort in the last eight contractual months could be aimed at further improvement in the composition or compositions of the high modulus non-beryllia containing glass fiber. This report details the research carried out under the contract and the test results obtained while examining the significance of the data reported.

## THE NEW GLASSES THAT WERE PREPARED AND THE REASONS FOR CHOOSING THESE COMPOSITIONS

### Earlier NASA Contracts for Glass Fiber Research at UARL

Contracts NASW-1301, NASW-2013, and NASW-2209 (Refs. 1,2) monitored by J. J. Gangler of NASA Headquarters and carried out over several years by the United Aircraft Research Laboratories concentrated on the study of the kinetics of crystallization of molten oxide systems which form complex three-dimensional crystal structures. Typical examples of such structures are beryl, cordierite, and benitoite, all of which are silicates. Beryl, for example, is $Be_3Al_2Si_6O_{18}$ requiring that 29 atoms meet in a common location and have a crystal structure possessing rings of ions arranged in sheets with their planes parallel and with the metal ions lying between these sheets and binding the rings together. When such ring structures are heated in a melt, the rings tend to open and link up into extended chains. Then, if the melt is quickly cooled, the rings do not have time to reform and a glass results. If the metal ions continue to bind the extended chains together, the possibility of cross-linked chains or polymer formation exists which will greatly stiffen the structure compared to a normal glass chain and could give rise to the high modulus of elasticity observed for numbers of the new UARL glasses.

One of the more outstanding high modulus cordierite-rare earth-beryl system glasses developed from these concepts is the glass composition UARL 344. Intensive investigation of this composition showed that it could be readily fiberized and fibers can be continuously drawn at high rates of speed and restarted at will. Over a quarter billion feet of these fibers have been drawn through an orifice of 0.038 in. diameter (platinum-20 percent rhodium bushing) at orifice temperatures of 1260°C to 1310°C, with beads of molten glass from 3/8 in. to 1 1/2 in., and at winding speeds of 4000 to 8000 ft/min (the top speed of our winder). The glass fibers processed under these conditions show excellent properties. Diameters vary from 0.2 to 0.4 mils with a Young's modulus of 18.6 psi, a specific modulus of 1.57 million inches, and strengths which, in twenty-two consecutive measurements, averaged 772,000 psi and ranged from 600,000 to 1,000,000 psi with a few extreme values discarded. With these properties, UARL scientists calculated for a 70 percent volume to glass fiber resin matrix with $\pm 45°$ alignment, the results should be

| Fiber | Density lbs/in | Modulus million psi | Specific Modulus ten million inches |
|---|---|---|---|
| E | 0.0776 | 3.27 | 4.21 |
| S | 0.0762 | 4.12 | 5.41 |
| UARL 344 | 0.0951 | 6.08 | 6.39 |

and these properties are fully realized, thus making such matrices useful for spar and shell blades, torque tubes, and rotary machinery in general.

## Non-Beryllia High Modulus Glasses Prepared Under Current NASA Contract

The current NASA contract for glass fiber research at UARL is NAS1-11648 and has as its purpose the elimination of the beryllia content from the several existing high moduli glasses just discussed which had been developed under the earlier NASA contracts without appreciable decrease in modulus. The approach to this program has included a detailed review of all previous non-beryllia high moduli glasses that could be fiberized. These fiberizable non-beryllia glasses are assembled in Table I together with composition and property data. The table shows UARL 321 to have the highest fiber modulus but this glass can be mechanically drawn only under very special conditions. The second highest modulus glass fiber in the table is that drawn from UARL 237 but the large statistical error makes this data questionable. It would, therefore, appear that UARL 129 is the most outstanding non-beryllia glass that could be fiberized at the time the contract was initiated.

UARL 129 was consequently chosen for large scale studies. By now more than 100 million feet of this non-beryllia glass have been produced as monofilament without any difficulty. The glass fiber consistently shows a Young's modulus of 16.7 million psi, a density of 3.24 gms/cm$^3$ and a strength measured on pristine uncoated and unhandled monofilament of 669,000 psi or 0.461 meganewtons/cm$^2$ as the result of averaging 28 consecutive strength determinations. This group of strength measurements ranged from 476,000 psi to 819,000 psi with six consecutive measurements varying only from 726,666 psi to 756,756 psi. UARL 129 glass fiber can be produced equally well as monofilament with a speed of 6000 ft per minute and a diameter of 0.3 mil or at a lower speed of 2100 ft per minute with a resultant diameter of 0.85 to 0.9 mil. UARL 129 fiber can also be readily sized and added to an epoxy-resin matrix where it shows a retained specific strength 12 percent greater than that of Ferro's "S" glass in composites made similarly in this laboratory.

| Glass | Density of Composite Fiber Content 50% by Volume | Strength of Composite Fiber Content 50% by Volume | Relative Specific Strength |
|---|---|---|---|
| Ferro "S" | 1.76 gms/cm$^3$ | 197,000 psi | 1.00 |
| UARL 129 | 2.24 gms/cm$^3$ | 282,000 psi | 1.12 |

At the time that large quantities of UARL 129 glass were fabricated as monofilaments and then used to form unidirectional composites for evaluation, the search was continued for a new non-beryllia glass of higher modulus and strength as a part-time (25 percent) effort. The properties and compositions of the glasses originated at this time are shown in Table II. The most interesting

Table I

Characterization of Non-Beryllia Modulus Glasses That Can Be Fiberized

| Glass | Bulk Modulus MN/cm$^2$ | Bulk Modulus ($10^6$psi) | Molal Sum | Density gms/cm$^3$ | Fiber Modulus (sonic) MN/cm$^2$ | Fiber Modulus (sonic) ($10^6$psi) | Fiber Modulus (Instr) MN/cm$^2$ | Fiber Modulus (Instr) ($10^6$psi) | Uncertainty MN/cm$^2$ | Uncertainty ($10^6$psi) | $SiO_2$ | $Al_2O_3$ | MgO | $Y_2O_3$ | ZnO | $Li_2O$ | CaO | $Be_2O_3$ | $ZrO_2$ | Other Elements |
|---|---|---|---|---|---|---|---|---|---|---|---|---|---|---|---|---|---|---|---|---|
| 40 | 10.7 | 15.5 | | 2.98 | | | 11.2 | 16.2 | 3.17 | 4.6 | 58.4 | 20.9 | 16.3 | | | | | | | 4.53 $Ce_2O_3$ |
| 62 | 9.8 | 14.2 | | 2.74 | | | 9.6 | 14.0 | | | 54.6 | 15.2 | 29.2 | | | | | | | 1.0 $Ce_2O_3$ |
| 63 | | | | | | | 9.0 | 13.0 | | | 54.6 | 15.6 | 28.9 | | | | | | | 0.95 $La_2O_3$ |
| 64 | | | | | | | 10.1 | 14.7 | | | 54.6 | 15.5 | 28.8 | 1.39 | | | | | | |
| 65 | | | | | | | 9.5 | 13.8 | | | 54.6 | 15.6 | 28.9 | | | | | | | 0.89 $Sm_2O_3$ |
| 66 | | | | | | | 10.1 | 14.6 | 1.38 | 2.0 | 53.7 | 15.3 | 28.3 | | | | | | | 2.56 $ZrO_2$ |
| 67 | 9.9 | 14.4 | | 2.65 | | | 8.8 | 12.7 | | | 54.7 | 15.3 | 29.3 | | | | | | | 0.76 $Ta_2O_5$ |
| 68 | 9.7 | 14.1 | | 2.63 | | | 9.4 | 13.7 | | | 53.4 | 18.3 | 28.8 | | | | | | | |
| 69 | 9.8 | 14.2 | | 2.59 | | | 9.4 | 13.6 | | | 57.3 | 14.6 | 28.0 | | | | | | | |
| 70 | | | | | | | 9.2 | 13.4 | | | 55.3 | 12.6 | 29.3 | 2.83 | | | | | | |
| 71 | | | | | | | 9.4 | 13.7 | | | 49.4 | 14.1 | 36.5 | | | | | | | |
| 72 | 9.6 | 14.0 | | 2.89 | | | 8.6 | 12.5 | | | 56.9 | 15.1 | 25.4 | | | | | | | 2.60 $Ce_2O_3$ |
| 73 | | | | | | | 10.4 | 15.1 | | | 59.1 | 8.7 | 26.4 | 3.13 | | | | | | 2.70 $Ce_2O_3$ |
| 74 | | | | | | | 9.5 | 13.8 | | | 56.1 | 9.6 | 30.0 | 4.3 | | | | | | |
| 114 | 11.5 | 16.7 | | 3.22 | | | 10.4 | 15.1 | | | | | | | | | | | | |
| 126 | 11.6 | 16.8 | | 3.46 | | | 11.2 | 16.2 | 1.17 | 1.7 | | | | | | | | | | |
| 127 | 11.1 | 16.1 | | 3.25 | | | 10.5 | 15.2 | | | 60.0 | 10.0 | 20.0 | 10.0 | | | | | | |
| 129 | 11.4 | 16.5 | | 3.30 | | | 11.5 | 16.7 | 1.86 | 2.7 | 50.0 | 13.3 | 26.7 | 10.0 | | | | | | |
| 131 | 9.6 | 14.0 | | 3.14 | | | 8.6 | 12.5 | | | 70.0 | 6.7 | | 10.0 | | | 13.3 | | | |
| 136 | 9.9 | 14.4 | | 2.80 | | | 9.3 | 13.5 | | | 53.3 | 15.6 | 28.9 | | | | | | | 2.00 $La_2O_3$ |
| 137 | 9.2 | 13.3 | | 3.08 | | | 9.6 | 13.9 | | | 51.3 | 15.6 | 28.9 | | | | | | | 4.00 $La_2O_3$ |
| 138 | 10.5 | 15.3 | | 3.55 | | | 8.4 | 12.2 | | | 47.3 | 15.6 | 28.9 | | | | | | | 8.00 $La_2O_3$ |
| 140 | 10.8 | 15.6 | | 3.68 | | | 10.3 | 15.0 | | | 47.3 | 15.6 | 27.9 | | | | | | | 1.00 $Ce_2O_3$, 8.00 $La_2O_3$ |
| 155 | 10.8 | 15.7 | | 3.55 | | | 10.1 | 14.7 | 1.31 | 1.9 | 49.4 | 7.1 | 36.5 | | | | | | | 7.05 $Ta_2O_5$ |
| 157 | 9.2 | 13.3 | | 2.69 | | | 9.0 | 13.1 | 1.93 | 2.8 | 49.4 | 7.1 | 36.5 | | | | | | | 7.05 $V_2O_5$ |
| 159 | 11.2 | 16.2 | | 3.22 | | | 10.8 | 15.7 | 2.48 | 3.6 | 57.4 | 6.6 | 28.0 | 8.0 | | | | | | |
| 160 | | | | | | | 10.1 | 14.6 | 2.07 | 3.0 | 57.4 | 6.6 | 28.0 | | | | | | | 8.0 $La_2O_3$ |
| 161 | | | | | | | 9.8 | 14.3 | 1.24 | 1.8 | 57.4 | 6.6 | 28.0 | | | | | | | 8.0 $Re_2O_3$ |
| 166 | 8.6 | 12.5 | | 2.62 | | | 9.4 | 13.6 | 3.72 | 5.4 | 51.7 | 23.0 | 18.3 | | | | | | | 7.0 $V_2O_5$ |
| 175 | 11.1 | 16.1 | | 3.19 | | | 9.0 | 13.1 | 2.00 | 2.9 | 60.0 | 5.0 | 20.0 | 10.0 | | | | | | 5.0 $V_2O_5$ |
| 176 | 10.5 | 15.2 | | 3.14 | | | 11.5 | 16.7 | 6.82 | 9.9 | 70.0 | 3.7 | 13.3 | 10.0 | | | | | | 3.0 $V_2O_5$ |
| 193 | | | | | | | 9.0 | 13.1 | 2.76 | 4.0 | 49.4 | 6.1 | 28.5 | 5.0 | | | | | | 5.0 $La_2O_3$, 6.0 $V_2O_5$ |
| 200 | | | | | | | 10.1 | 14.6 | 2.28 | 3.3 | 48.0 | 13.3 | 26.7 | 6.0 | | | | | | 6.0 $La_2O_3$ |
| 201 | | | | | | | 9.1 | 13.2 | 2.96 | 4.3 | 48.0 | 13.3 | 26.7 | 6.0 | | | | | | 6.0 $Ce_2O_3$ |
| 210 | | | | | | | 10.3 | 15.0 | 1.38 | 2.0 | 48.0 | 13.3 | 26.7 | | | | | | | 10.0 $La_2O_3$ |

Table I (Cont'd)

| Glass | Bulk Modulus MN/cm$^2$ | Bulk Modulus ($10^6$psi) | Molal Sum | Density gms/cm$^3$ | Fiber Modulus (sonic) MN/cm$^2$ | Fiber Modulus (sonic) ($10^6$psi) | Fiber Modulus (Instr) MN/cm$^2$ | Fiber Modulus (Instr) ($10^6$psi) | Uncertainty MN/cm$^2$ | Uncertainty ($10^6$psi) | $SiO_2$ | $Al_2O_3$ | MgO | $Y_2O_3$ | ZnO | $Li_2O$ | CaO | $Be_2O_3$ | $ZrO_2$ | Other Elements |
|---|---|---|---|---|---|---|---|---|---|---|---|---|---|---|---|---|---|---|---|---|
| 214 | | | | | | | 8.9 | 12.9 | 1.10 | 1.6 | 60.0 | 6.0 | 34.0 | | | | | | | |
| 215 | | | | | | | 9.2 | 13.3 | 2.07 | 3.0 | 44.8 | | 4.5 | | | | | | | |
| 233 | 11.0 | 15.9 | | 3.03 | 10.3 | 14.9 | 10.1 | 14.6 | 1.58 | 2.3 | 50.0 | 13.3 | 26.7 | 5.0 | | | | | | |
| 235 | 12.0 | 17.4 | | 3.33 | | | 10.5 | 15.3 | 1.31 | 1.9 | 50.0 | 10.0 | 30.0 | 10.0 | | | | | | |
| 237 | 12.6 | 18.3 | | 3.33 | | | 13.0 | 18.8 | 5.45 | 7.9 | 45.0 | 15.0 | 30.0 | 10.0 | | | | | | |
| 231 | 12.5 | 18.1 | | 3.43 | | | | | | | 40.0 | 14.0 | 36.0 | 10.0 | | | | | | |
| 238 | 11.4 | 16.6 | | 3.04 | | | 10.5 | 15.2 | 2.21 | 3.2 | 45.0 | 15.0 | 30.0 | 5.0 | | | | | | |
| 279 | 8.5 | 12.4 | | 2.69 | | | 4.3 | 6.2 | 2.28 | 3.3 | | | | | | | | | | |
| 280 | 3.9 | 5.6 | | 2.05 | | | 3.2 | 4.6 | 0.28 | 0.4 | | | | | | | | | | |
| 284 | 10.3 | 14.9 | | 3.32 | | | 8.2 | 11.9 | 1.65 | 2.4 | 25.0 | 8.0 | 15.0 | | 8.0 | 15.0 | 2.0 | 10.5 | 2.0 | 7.0 $La_2O_3$, 7 CuO, 0.5 $Ce_2O_3$ |
| 285 | 10.4 | 15.1 | | 3.66 | | | 8.9 | 12.9 | 3.24 | 4.7 | 25.0 | 12.0 | 12.0 | | 12.0 | 12.0 | | 15.0 | | 12.0 $La_2O_3$ |
| 288 | 9.8 | 14.3 | | 3.60 | | | 8.2 | 11.9 | 1.93 | 2.8 | 25.0 | 12.0 | 12.0 | | 12.0 | 12.0 | | 15.0 | | 12.0 $La_2O_3$, 6 CuO |
| 289 | 10.3 | 15.0 | | 3.90 | | | 9.0 | 13.1 | 1.03 | 1.5 | 25.0 | 12.0 | 12.0 | | 12.0 | 12.0 | | 9.0 | | 12.0 $La_2O_3$, 6 CuO |
| 290 | 10.0 | 14.5 | | 3.24 | | | 9.8 | 14.3 | 4.00 | 5.8 | 25.0 | 8.0 | 15.0 | 7.0 | 15.0 | 15.0 | | 15.0 | | |
| 291 | 10.8 | 15.7 | | 3.32 | | | 9.4 | 13.6 | 2.21 | 3.2 | 25.0 | 12.0 | 12.0 | 12.0 | 12.0 | 12.0 | | 15.0 | | |
| 299 | 10.1 | 14.6 | | 3.18 | | | 8.8 | 12.8 | 2.48 | 3.6 | 25.0 | 8.0 | 15.0 | | | 15.0 | 15.0 | 15.0 | | 7.0 $La_2O_3$ |
| 300 | 10.0 | 14.5 | | 2.88 | | | 9.2 | 13.4 | 2.34 | 3.4 | 25.0 | | 15.0 | | 15.0 | 15.0 | 15.0 | 15.0 | | |
| 320 | 11.0 | 16.0 | | 2.93 | 11.2 | 16.2 | 12.8 | 18.6 | 2.28 | 3.3 | 45.0 | 15.0 | 30.0 | | | | | | 10.0 | |
| 396 | 10.5 | 15.2 | | 3.24 | 10.3 | 15.0 | 10.4 | 15.1 | 1.17 | 1.7 | 45.0 | 15.0 | 15.0 | | | 10.0 | | | 15.0 | |
| 402 | 12.3 | 17.8 | | 3.31 | 11.0 | 15.9 | 11.4 | 16.5 | 2.14 | 3.1 | 25.0 | 8.0 | 20.0 | 14.0 | | 5.0 | 9.0 | 14.0 | | 2.0 CuO, 3.0 $TiO_2$ |
| 403 | 11.8 | 17.2 | | 3.37 | 11.0 | 16.0 | 12.4 | 18.0 | 1.86 | 2.7 | 25.0 | 8.0 | 20.0 | 14.0 | | 5.0 | 6.0 | 14.0 | | 3 $Fe_2O_3$, 2.0 CuO, 3.0 $TiO_2$ |
| 321 | 12.9 | 18.7 | | 3.18 | 13.7 | 19.9 | 12.6 | 18.3 | 1.72 | 2.5 | 40.0 | 15.0 | 30.0 | 15.0 | | | | | | |
| 449 | 12.5 | 18.1 | | 3.39 | 10.9 | 15.8 | | | | | 25.0 | | 20.0 | 12.0 | 4.0 | 6.0 | 15.0 | 13.0 | | 2.0 CuO, 3.0 $TiO_2$ |
| 464 | 11.1 | 16.1 | | 3.07 | 10.2 | 14.8 | | | | | 25.0 | | 15.0 | 5.0 | 10.0 | 15.0 | 15.0 | 15.0 | | |
| 481 | 12.6 | 18.3 | 80.6 | 3.23 | 10.8 | 15.6 | | | | | 55.0 | 17.0 | 17.0 | 10.0 | | | | | | 1.0 CoO |
| 482 | 11.6 | 16.8 | 79.5 | 3.15 | 9.4 | 13.6 | | | | | 65.0 | 12.0 | 12.0 | 10.0 | | | | | | 1.0 CoO |
| 483 | 11.5 | 16.7 | 82.5 | 3.15 | 10.0 | 14.5 | | | | | 65.0 | 17.0 | 7.0 | 10.0 | | | | | | 1.0 CoO |
| 486 | 11.1 | 16.1 | 79.9 | 3.19 | 10.1 | 14.7 | | | | | 58.0 | 12.0 | 10.0 | 10.0 | | | 10.0 | | | |
| Several High Modulus Glasses Containing Beryllia That Can Be Fiberized | | | | | | | | | | | | | | | | | | | | |
| 344 | 14.0 | 20.3 | | 3.29 | 12.8 | 18.6 | | | | | 45.0 | 15.0 | 15.0 | 10.0 | | | | | | 15 BeO |
| 417 | 13.4 | 19.4 | | 3.09 | 12.1 | 17.5 | | | | | 45.0 | 15.0 | 15.0 | 7.0 | | | 3.0 | | | 15.BeO |
| 331 | 14.4 | 20.9 | | 3.66 | 13.6 | 19.8 | | | | | 39.0 | 12.0 | | 12.0 | 12.0 | | | | | 25 BeO |
| 405 | 13.6 | 19.7 | | 3.73 | 12.7 | 18.4 | | | | | 49.3 | 14.0 | | 22.0 | | | 0.7 | | | 14 BeO |
| Several High Modulus Glasses Without Beryllia That Can Not Be Fiberized | | | | | | | | | | | | | | | | | | | | |
| 383 | 15.7 | 22.75 | 64.9 | 3.14 | | | | | | | 24.0 | 3.0 | 16.0 | | 8.0 | 12.0 | 12.0 | 10.0 | 12.0 | 3 CuO |
| 270 | 14.0 | 20.3 | 70.13 | 3.53 | | | | | | | 25.0 | 8.0 | 15.0 | 7.0 | 15.0 | 15.0 | 15.0 | | | |
| 329 | 14.3 | 20.7 | | 3.03 | | | | | | | 22.2 | 11.1 | 22.2 | 11.1 | 11.1 | 11.1 | | | 11.1 | |
| 337 | 14.4 | 20.9 | | 3.94 | | | | | | | 30.0 | 15.0 | 30.0 | 12.5 | | | | | | |

Table II

Recently Developed Non-Beryllia Glasses Compared to UARL 129 Glass

| Glass | Bulk Modulus MN/cm² | Bulk Modulus ($10^6$psi) | Molal Sum | Density gms/cm³ | Fiber Modulus MN/cm² | Fiber Modulus ($10^6$psi) | $SiO_2$ | $Al_2O_3$ | MgO | $Y_2O_3$ | ZnO | $Li_2O$ | CaO | $B_2O_3$ | $ZrO_2$ | $Ce_2O_3$ | $La_2O_3$ | Other Ingredients | Bulk Modulus As Calc. MN/cm² | Bulk Modulus As Calc. ($10^6$psi) | Calc. OK |
|---|---|---|---|---|---|---|---|---|---|---|---|---|---|---|---|---|---|---|---|---|---|
| 497 | 12.8 | 18.6 | 70.6 | 3.38 | | | 40 | | 14 | 10 | | 12 | 18 | | | | | 4 $TiO_2$, 2 CoO | | | |
| 498 | 11.2 | 16.2 | 78.7 | 3.25 | | | 56 | 7.75 | | 10 | | 2 | 22.25 | | | | | 2 CoO | | | |
| 499 | 13.4 | 19.5 | 76.9 | 3.61 | | | 40 | 2.66 | 18 | 10 | | 2 | 16 | | 4 | | | 7 $TiO_2$, 1/3 CoO | | | |
| 500 | 13.1 | 18.97 | 79.1 | 3.59 | | | 30 | | 20 | 12 | | 3 | 15 | 8 | 3.66 | | | 8 $TiO_2$, 1/3 CoO | | | |
| 501 | 13.1 | 19.0 | 80.8 | 3.62 | | | 30 | | 20 | 12 | | 2 | 12 | 8 | 4.5 | | | 11 $TiO_2$, 1/2 CoO | | | |
| 502 | 13.1 | 19.0 | 90.1 | 3.89 | 9.4 | 13.6 | 45 | | 12 | 10 | | 2 | 12 | | 2 | | 2 | 10 $TiO_2$, 1 CoO, 4 $ThO_2$ | | | |
| 503 | 13.5 | 19.55 | 78.8 | 3.65 | | | 39 | | 15 | 10 | | 2 | 15 | | 6 | | | 12 $TiO_2$, 1 CoO | | | |
| 504 | | | 83.9 | 3.50 | | | 47 | 7 | 17 | 10 | | 3 | 10 | | | | | 6 $Cu_2O$, not prepared | | | |
| 505 | | | 78.8 | | | | 47 | 7 | 17 | 5 | | 3 | 10 | | 5 | | | 6 $Cu_2O$, gave free Cu | | | |
| 506 | | | 73.6 | 3.31 | | | 47 | 7 | 17 | 3 | | | 10 | | 10 | | | 6 $Cu_2O$, gave free Cu | | | |
| 507 | | | 73.6 | 3.35 | | | 47 | 7 | 7 | | 10 | 3 | 10 | 5 | 5 | | | 6 $Cu_2O$, gave free Cu | | | |
| 508 | 10.7 | 15.5 | 75.5 | 3.13 | 9.8 | 14.24 | 40 | 7 | 15 | 5 | 10 | 3 | 10 | 5 | 5 | | | | | | |
| 509 | 12.4 | 18.0 | 80.5 | 3.35 | 11.0 | 15.96 | 40 | 12 | 24 | 10 | 6 | 3 | | 3 | 2 | | | | | | |
| 510 | 12.0 | 17.4 | 80.3 | 3.45 | | | 35 | 12 | 27 | 10 | 8 | 3 | | 3 | 2 | | | | | | |
| 511 | 12.0 | 17.4 | 79.1 | 3.54 | | | 35 | 7 | 22 | 10 | 10 | 3 | 8 | 3 | 2 | | | | | | |
| 512 | 11.9 | 17.3 | 81.5 | 3.51 | 11.0 | 15.98 | 35 | 10 | 17 | 10 | 10 | 3 | 10 | 3 | 2 | | | | | | |
| 513 | 12.1 | 17.6 | 76.8 | 3.57 | | | 35 | 6 | 12 | 10 | 10 | 3 | 6 | 3 | 5 | | | | | | |
| 514 | 12.9 | 18.7 | 82.2 | 3.57 | | | 35 | 11 | 23 | 10 | 12 | 3 | | 3 | 3 | | | | 13.4 | 19.5 | No |
| 515 | 13.0 | 18.9 | 89.6 | 3.67 | | | 42 | 5 | 25 | 12 | 3 | 4 | | | 6 | | | | 13.1 | 19.0 | Yes |
| 516 | 12.9 | 18.76 | 80.0 | 3.61 | | | 42 | | 25 | 12 | 3 | 4 | 5 | 3 | 6 | | | | 13.1 | 18.96 | Yes |
| 517 | 10.9 | 15.8 | 81.7 | 3.14 | | | 25 | | 15 | 10 | 10 | 10 | 15 | 15 | | | | | 12.3 | 17.8 | No |
| 518 | 11.2 | 16.3 | 86.4 | 3.26 | | | 25 | | 15 | 10 | 10 | 5 | 15 | 15 | 5 | | | | 13.1 | 19.0 | No |
| 519 | 13.0 | 18.8 | 83.6 | 3.64 | | | 50 | 12 | 15 | 12 | 5 | 3 | | | 2 | | | 1 CoO | 12.5 | 18.2 | No |
| 520 | | | 74.7 | | | | 50 | | 20 | 12 | | 3 | 14 | | | | | 1 CoO | | Can't Melt | |
| 521 | 12.2 | 17.7 | 76.0 | 3.28 | | | 50 | 12 | 22 | 10 | | 5 | | | | | | 1 CoO | 11.4 | 16.6 | Yes |
| 522 | 12.8 | 18.6 | 75.6 | 3.75 | | | 45 | 13 | 26 | 10 | | 5 | | | | | | 1 CoO | 11.8 | 17.1 | No |
| 523 | 12.3 | 17.8 | 83.6 | 3.39 | | | 45 | 17 | 17 | 10 | | 5 | | | | | | 1 CoO, 5 $SnO_2$ | | | |
| 524 | 11.9 | 17.3 | 79.1 | 3.54 | | | 25 | | 15 | 12 | 8 | 7 | 15 | 13 | | | | 3 $TiO_2$, 2 CuO | 13.2 | 19.1 | No |
| 525 | 12.3 | 17.9 | 76.1 | | | | 44 | 10 | 30 | 10 | 5 | | | | | | | 1 CoO | 12.3 | 17.8 | Yes |
| 526 | 12.5 | 18.2 | 75.2 | | | | 45 | 13 | 27 | 10 | | 5 | | | | | | | 11.8 | 17.2 | Yes |
| 527 | 11.7 | 17.0 | 76.0 | 3.31 | 11.4 | 16.6 | 45 | 10 | 30 | 10 | 5 | | | | | | | | 12.5 | 18.1 | No |
| 528 | 11.8 | 17.1 | 71.8 | 3.23 | | | 45 | 10 | 22 | 8 | | 3 | 12 | | | | | | | | |
| 529 | 11.5 | 16.7 | 75.9 | 3.39 | | | 45 | 10 | 22 | 4 | | 3 | 12 | | | 4 | | | | | |
| 530 | 11.3 | 16.4 | 75.9 | 3.35 | | | 45 | 10 | 22 | 4 | | 3 | 12 | | | | 4 | | | | |
| 531 | 11.0 | 15.9 | 80.0 | 3.45 | | | 45 | 10 | 22 | | | 3 | 12 | | | 8 | | | | | |
| 532 | 10.9 | 15.8 | 79.8 | 3.47 | | | 45 | 10 | 22 | | | 3 | 12 | | | | 8 | | | | |
| 533 | 11.8 | 17.2 | 86.7 | 3.72 | | | 45 | 10 | 20 | 4 | | 3 | 10 | | | 4 | 4 | | | | |
| 534 | 11.8 | 17.1 | 77.2 | 3.57 | | | 45 | 10 | 20 | 4 | 4 | 3 | 10 | | | 4 | | | | | |
| 535 | 11.5 | 16.7 | 77.1 | 3.38 | | | 45 | 10 | 20 | 4 | 4 | 3 | 10 | | | | 4 | | | | |
| 536 | 11.2 | 16.3 | 75.9 | 3.24 | 10.2 | 14.75 | 51.5 | 11.3 | 25.1 | 4.5 | | 3.5 | | | | | 4.5 | | | | |
| 537 | 11.0 | 15.9 | 80.0 | 3.46 | | | 45 | 10 | 22 | | | 3 | 12 | | | | 8 | 4.5 $Re_2O_3$ | | | |
| 538 | 10.8 | 15.6 | 75.9 | 3.24 | 10.6 | 15.46 | 51.5 | 11.3 | 25.1 | 4.5 | | 3.5 | | | | | | 4.5 $Re_2O_3$ | | | |
| 539 | 11.2 | 16.3 | 80.0 | | | | 45 | 10 | 22 | | | 3 | 12 | | | | | 8 $Re_2O_3$ | | | |
| 540B | 11.9 | 17.3 | | | | | 24.55 | | | 8.16 | | | | 21.18 | 10.45 | | 29.4 | 6.25 $Ta_2O_5$ | | | |
| 129 | 11.4 | 16.5 | | 3.28 | 11.5 | 16.7 | 50 | 13.3 | 26.7 | 10 | | | | | | | | | | | Yes |

of these new glasses is probably UARL 529 and this glass is compared with UARL 129 and a rediscovered glass, UARL 481, from Table III.

Table III

Young's Modulus of Several Non-beryllia Glass Fibers

| Glass | Bulk Modulus $10^6$ psi | Density gms/cm$^3$ | Fiber Modulus $10^6$ psi | Ratio of Fiber Modulus to Density $10^6$ psi/gms/cm$^3$ |
|---|---|---|---|---|
| UARL 129 | 16.5 | 3.29 | 16.45 | 5.00 |
| UARL 481 | 18.0 | 3.23 | 16.15 | 5.00 |
| UARL 529 | 16.7 | 3.31 | 16.55 | 5.00 |
| Ferro "S" | | 2.48 | 12.4 | 5.00 |

The UARL 529 glass can be produced at marked savings compared to UARL 129 because it has only forty percent as much yttria, the most expensive ingredient in the batch. The UARL 481 glass fiber, on the other hand, costs the same as the UARL 129 fiber to produce but is easier to fiberize at high speeds. UARL 481 bulk glass also has an advantage compared to UARL 129 since it has a Young's modulus for bulk specimens almost two million psi larger than its fiber modulus whereas for UARL 129 glass bulk and fiber moduli are equal. In the case of UARL 481, therefore, it is conceptually possible to improve the modulus of the glass fiber as much as 5 to 10 percent by heat treatment while the fiber is being drawn.

Detailed analyses of all the glass compositions prepared to date by UARL such as those shown in Tables I and II and in earlier reports (Ref. 1) proved that it is possible to predict in many cases with a high degree of accuracy the modulus to be expected from a given set of ingredients. This prediction is based on an extension of the work of C. J. Phillips (Ref. 6). In this article Dr. Phillips describes a method of calculating Young's modulus of elasticity for some 44 glasses by expressing the amount of each oxide present in mol percent and multiplying it by a modulus factor peculiar to that oxide. The coefficients he derives, however, are only for certain oxides such as $SiO_2$, $Na_2O$, $K_2O$, $Li_2O$, $B_2O_3$, $Al_2O_3$, CaO, MgO, PbO, BaO, ZnO and BeO likely to be present in the usual glasses. The numerical value of Young's modulus is then the sum of the terms

$$C_1P_1 + C_2P_2 + C_3P_3 + \ldots C_nP_n$$

where the $C_1 \ldots C_n$ are molal coefficients and $P_1 \ldots P_n$ are the molar percentages of the corresponding oxides. In our work we have determined these coefficients for a number of additional less common oxides by measuring the modulus of each experimental glass produced and analysis of the result in terms of its composition. The data collected to date is shown in Table IV and the accuracy that can be achieved using this data to predict the modulus of a new experimental glass is

Table IV

Summary of All Experimentally Determined Molar Modulus Coefficients and Some Examples of Their Use

A. Summary of All Experimentally Determined Molar Modulus Coefficients

| Oxide | Contribution Per Mol (kilobars) | Oxide | Contribution Per Mol (kilobars) |
|---|---|---|---|
| $SiO_2$ | 7.3 | ZnO | 20.0 |
| $Al_2O_3$ | 12.1 | $ZrO_2$ | 23.8 |
| CaO | 11.45 | MgO | 13.64 |
| $Li_2O$ | 7.0 | $Ce_2O_3$ | 19.6 |
| $B_2O_3$ | 7.2 | $Y_2O_3$ | 28.6 |
| $TiO_2$ | 15.0 | $Ta_2O_5$ | 19.4 |
| BeO | 19.0 | $La_2O_3$ | 18.6 |
| | | CoO | 11.0 |

B. Comparison of Calculated & Experimental Moduli for UARL 471 Glass

| Constituent | Mol % | Kilobars/Mol | Contributions |
|---|---|---|---|
| $SiO_2$ | 25 | 7.3 | 183 |
| $Al_2O_3$ | 8 | 12.1 | 97 |
| MgO | 15 | 13.64 | 200 |
| $Li_2O$ | 15 | 7.0 | 105 |
| CaO | 10 | 11.45 | 115 |
| ZnO | 15 | 20.0 | 300 |
| $Y_2O_3$ | 7 | 28.6 | 200 |
| $B_2O_3$ | 5 | 7.2 | 36 |
| | | | 1241 kilobars calc. |

But experimentally UARL 471 glass has a modulus - $17.90 \times 10^6$ psi = 1235 kilobars

C. Calculation (in advance of preparation) of Modulus to be Expected from UARL 500 Glass

| Constituent | Mol % | Kilobars/Mol | Contributions |
|---|---|---|---|
| $SiO_2$ | 30 | 7.3 | 219 |
| MgO | 20 | 13.64 | 273 |
| $Li_2O$ | 3 | 7.0 | 21 |
| CaO | 15 | 11.45 | 172 |
| $Y_2O_3$ | 12 | 28.6 | 343 |
| $B_2O_3$ | 8 | 7.2 | 58 |
| $TiO_2$ | 8 | 15 | 120 |
| $ZrO_2$ | 3.66 | 23.8 | 87 |
| CoO | 0.33 | 11 | 4 |
| | | | 1297 kilobars calc. |

But the UARL 500 glass when made actually had a modulus = $18.97 \times 10^6$ psi = 1309 kilobars

shown in Table IV. The surprisingly high values found for the contributions of zinc oxide and tantalum oxide to Young's modulus opens the door to the production of many new high-modulus non-beryllia glasses where these oxides are purposely added to the basic four component system of cordierite and rare-earth oxide used to produce UARL 129, 481 and 529. The effect of each such addition on viscosity, surface tension, fiberizability, density, and strength must, of course, be measured. Also, other four component basic systems may need to be substituted before the optimum composition for incorporation of these new high modulus oxides is fully successful.

## METHOD OF MAKING UNIDIRECTIONAL FIBER REINFORCED EPOXY RESIN COMPOSITES

Several variations of procedure were necessary before satisfactory unidirectional UARL glass fiber-epoxy resin composites could be prepared from monofilament glass fiber in order to form the necessary samples for physical evaluation. Initially these composites were formed in this manner. One million eight hundred thousand lineal feet of UARL 129 fiber were produced by drawing the glass through a single-hole platinum-rhodium bushing at a speed of 6000 feet per minute. Before reaching the drawing (winding) drum, the glass fiber contacted a sizing applicator (which applied 237B size, a coupling agent-lubricant combination) and then was partially dried by passing through a six inch long cylindrical furnace whose temperature was 350°C. After leaving this furnace, the fiber contacted a finish applicator (which applied MPG8-80 finish prepared by dissolving 25 gms of coupling agent A-187, 5 gms of Union Carbide resin ERL 2256 epoxy resin, and 1.35 gms of 0820 curing agent in 94 gms of diacetone alcohol) and then passed through a second cylindrical furnace maintained at a temperature of 450°C. Finally, the sized and finished glass fiber was gathered on a winding drum.

The winding drum is covered with a cardboard cylinder and this cylinder is then lined with Mylar tape. The paper spool is 12 1/2 in. in diameter and the glass fiber winding on it is 3 1/2 in. in width. Tape is then formed from the sized UARL 129 glass fiber monofilament by brushing it twice with a fifty percent solution of Union Carbide resin ERL 2256-0820. The tape is next cut into 9 1/2 in. lnegths and dried at 100°C for twenty minutes. Then each ply is laid up in the mold to the desired thickness and subjected to contact pressure from the mating surface of the mold. At this time it is heated to 80°C and remains under these conditions until gelation, usually about forty minutes. After gelation it is pressed at 200 psi and 80°C for 80 minutes. Finally, it is postcured while in the mold but outside of the press at a temperature of 150°C for two hours and allowed to cool to room temperature while still in the mold. The specimens are then removed from the mold, trimmed, and cut to desired test size.

Rigid adherence to this procedure of sample preparation yielded only very unsatisfactory composites like those shown in Table V. Here, the satisfactory composites are obvious from the parameters. The unuseable composites were in general characterized by too high a density, too high a percentage of glass fiber, excessive voids, black streaks, non-uniform fiber dispersion, and surface defects.

Table V

Parameters of Experimental Epoxy Resin-Fiber Composites Prepared at UARL

| Composite Number | Fiber Used | Purpose | Parameters of the Composite | | | | |
|---|---|---|---|---|---|---|---|
| | | | Density gms/cm$^3$ | % Fiber #1 | % Fiber #2 | % Resin | % Voids |
| 396-4 | UARL 129 | Tensile | 2.73 | 72.7 | none | 26.8 | 1.00 |
| 396-5 | UARL 129 | Tensile | 2.69 | 74.0 | none | 20.3 | 5.8 |
| 396-9 | UARL 129 | Short Beam | 2.62 | 70.0 | none | 25.1 | 4.9 |
| 396-10 | UARL 129 | Short Beam | 2.69 | 69.0 | none | 21.0 | 10.1 |
| 396-11 | UARL 129 | Fatigue | 2.75 | 74.3 | none | 23.8 | 1.8 |
| 396-12 | UARL 129 | Fatigue | 2.71 | 76.2 | none | 15.6 | 8.2 |
| 396-13 | UARL 129 | Fatigue | 2.79 | | none | | |
| 396-14 | UARL 129 | Fatigue | 2.79 | 76.1 | none | 22.4 | 1.5 |
| 396-16 | UARL 129 | Fatigue | 2.60 | 68.5 | none | 30.0 | 1.65 |
| 396-17 | UARL 129 | Fatigue | 2.74 | 73.3 | none | 23.7 | 2.9 |
| 396-19 | Thornel 75S | Tensile | 1.43 | 39.1 | none | 58.2 | 2.7 |
| 396-20 | UARL 129 | Fatigue | 2.50 | 64.0 | none | 34.6 | 1.39 |
| 396-21 | UARL 129 | Compression | 2.50 | 62.3 | none | 35.9 | 1.8 |
| 396-23 | UARL 129 | Tensile | 2.30 | 50.7 | none | 53.1 | neg. |
| 396-25 | UARL 129 | Tensile | 2.28 | 50.2 | none | 49.8 | 0.04 |
| 396-26 | UARL 129 | Fatigue | 2.43 | 55.3 | none | 41.8 | 4.03 |
| 396-28 | Thornel 75S | Tensile | 1.40 | 41.1 | none | 52.6 | 6.4 |
| 396-29 | Thornel 75S | Tensile | 1.44 | 40.6 | none | 56.4 | 3.0 |
| 396-30 | UARL 129 | Fatigue | 2.44 | 61.9 | none | 29.3 | 8.8 |
| 396-31 | Thornel 75S | Tensile | 1.44 | 31.4 | none | 62.9 | 1.6 |
| 396-34 | UARL 129 | Fatigue | 2.30 | 53.6 | none | 44.7 | 2.70 |
| 396-35 | UARL 129 | Fatigue | 2.52 | 66.5 | none | 29.9 | 3.74 |
| 396-36 | UARL 129 | Fatigue | 2.51 | 63.5 | none | 36.4 | 0 |
| 396-39 | UARL "S" | Tensile | 1.84 | 46.3 | none | 52.1 | 1.2 |
| 396-40 | UARL "S" | Fatigue | 1.87 | 50.9 | none | 46.6 | 2.5 |
| 396-41 | UARL "S" | Fatigue | 1.89 | 52.1 | none | 47.3 | 0.5 |
| 396-42 | UARL "S" | Fatigue | 1.91 | 53.6 | none | 47.4 | 0 |
| 396-43 | UARL "S" | Fatigue | 1.84 | 48.2 | none | 51.7 | 0 |
| 396-44 | UARL "S" | Fatigue | 1.77 | 42.7 | none | 57.3 | 0 |
| 396-50 | UARL 129 | Creep | 2.56 | 65.9 | none | 31.1 | 3.0 |
| 396-51 | UARL 129 | Tensile | 2.60 | 67.5 | none | 32.8 | neg. |
| 396-52 | UARL 129 | Tensile | 2.38 | 56.7 | none | 43.8 | neg. |
| 396-53 | UARL 129 | Short Beam | 2.60 | 69.6 | none | 31.5 | neg. |
| 396-54 | UARL 129 | Short Beam | 2.51 | 63.0 | none | 38.2 | neg. |
| 396-55 | UARL 129 | Compression | 2.48 | 62.4 | none | 36.8 | 0.758 |
| 396-56 | UARL "S" | Tensile | 2.04 | 62.0 | none | 40.0 | neg. |
| 396-57 | UARL "S" | Tensile | 2.02 | 61.0 | none | 40.6 | neg. |
| 396-58 | UARL "S" | Short Beam | 1.99 | 59.2 | none | 41.5 | neg. |
| 396-59 | UARL "S" | Short Beam | 2.08 | 67.0 | none | 34.2 | neg. |
| 396-60 | UARL "S" | Compression | 2.03 | 62.9 | none | 38.8 | neg. |
| 396-61 | Thornel 75S | Tensile | | | none | | |
| 396-62 | Thornel 75S | Tensile | 1.50 | 41.5 | none | 60.0 | neg. |
| 396-63 | Thornel 75S | Tensile | 1.49 | 41.7 | none | 58.9 | 0 |
| 396-64 | Thornel 75S | Tensile | 1.56 | 53.5 | none | 47.1 | 0 |
| 396-65 | Thornel 75S | Tensile | 1.61 | 63.7 | none | 36.3 | 0 |
| 396-66 | Thornel 75S | Short Beam & Fat. | 1.56 | 56.2 | none | 43.5 | 0.3 |
| 396-67 | Thornel 75S | Short Beam & Fat. | 1.56 | 54.2 | none | 44.5 | 1.35 |
| 396-68 | Thornel 75S | Compression | 1.58 | 57.0 | none | 44.0 | neg. |
| 396-69 | Thornel 75S, UARL 129 | Tensile | 2.12 | 27.8Gr | 34.2Gl | 40.7 | neg. |
| 396-70 | Thornel 75S, UARL 129 | Tensile | 2.11 | 33.0Gr | 32.4Gl | 37.4 | neg. |
| 396-71 | Thornel 75S | Fatigue | 1.58 | 57.2 | none | 43.4 | neg. |
| 396-72 | Thornel 75S, UARL 129 | Short Beam & Fat. | 2.00 | 29.9Gr | 29.6Gl | 40.3 | 0.35 |
| 396-73 | Thornel 75S, UARL 129 | Short Beam & Fat. | 2.05 | 32.6Gr | 30.9Gl | 37.0 | 0 |
| 396-74 | Thornel 75S, UARL 129 | Short Beam & Fat. | 1.96 | 26.6Gr | 26.5Gl | 49.9 | neg. |
| 396-75 | UARL 129, Thornel 75S | Tensile | 2.14 | 37.6Gl | 26.5Gr | 35.9 | 0.16 |
| 396-76 | UARL 129, Thornel 75S | Tensile | 2.10 | 34.6Gl | 30.6Gr | 34.0 | 0.746 |
| 396-77 | UARL 129, Thornel 75S | Short Beam & Fat. | 2.13 | 37.6Gl | 25.5Gr | 36.4 | 0.455 |
| 396-78 | UARL 129, Thornel 75S | Short Beam & Fat. | 2.02 | 33.0Gl | 27.7Gr | 35.9 | 3.45 |
| 396-79 | Thornel 75S | Fatigue | 1.53 | 53.8Gr | none | 44.7 | 1.58 |
| 396-80 | UARL 129, Thornel 75S | Short Beam & Fat. | 2.19 | 40.9Gl | 25.5Gr | 32.1 | 1.32 |
| 396-81 | UARL 129, Thornel 75S | Compression | 2.25 | 43.0Gl | 25.6Gr | 31.8 | neg. |
| 396-82 | Thornel 75S, UARL 129 | Compression | 2.07 | 30.6Gr | 33.9Gl | 33.6 | 2.06 |
| 111 | UARL "S" | Creep | 1.90 | 53.7 | | 46.0 | 0.387 |

Gl = glass  Gr = graphite = Thornel 75S

The satisfactory composites of Table V were produced by a number of changes in operating procedure. The cylindrical furnaces were eliminated and with them went the black streaks. Only the first coating or size was applied while the fiber was being drawn and it was dried with a hot air gun after the spool was removed from the winder. The second coating or finish (MPG8-80 finish) was applied by brushing the solution on the detached spool. The amount of fiber on each individual drum was reduced to 900,000 ft and the mold was more carefully cleaned. The remainder of the procedure was followed without change except that after the plies were first laid in the mold and the mold closed, 5 psi pressure was applied.

## THE METHODS USED TO EVALUATE THE MONOFILAMENT UNIDIRECTIONAL FIBER EPOXY RESIN COMPOSITES

The unidirectional fiber-epoxy resin composites prepared from glass monofilaments and/or Thornel 75S continuous twisted graphite fiber as described in the preceding section and as shown in Fig. 1 were next subjected to physical tests conducted in the following manner.

### Tensile Strength and Modulus Procedures for Composites

Tensile properties of the several glass fiber-epoxy resin matrix composites were evaluated as shown in Table VI. These tests at 0° to the filament direction were by far the more difficult to conduct because the high tensile strength and relatively low shear strength of the composites in that orientation frequently led to shear failures rather than tensile failures. Several specimen configurations were evaluated before the one shown in Fig. 2 was selected. In order to avoid shear failure in the shoulder of the specimen and to prevent the specimen from pulling out of the aluminum tabs, it was necessary to maximize the ratio of specimen length bonded between tabs to cross-sectional area of the specimen. Increasing the width of the specimen in the tabs had no beneficial effect because the specimens would split along a path the same width as the reduced width in the center. Since the specimen length was initially limited to 6 in. by fabrication facilities, the length of specimen which could be bonded to tabs was restricted to approximately 2 in. each end. Thus the small cross-sectional width shown in Fig. 2 was necessary to maximize the bond length: cross-sectional area ratio for the specimen. Unidirectional composites tested at 0° to the filament direction are apparently relatively insensitive to surface effects, so the small area of the specimen had no adverse effect on the test results. Tensile modulus at 0° to the filament direction was determined by testing a straight-sided bar. The bar was loaded to approximately 20 percent of its ultimate strength, then unloaded and machined into two tensile strength specimens. Strength values determined from those specimens were compared with values obtained from specimens which were not tested for modulus prior to testing to failure. The results were in good agreement which indicated that the determination of modulus was a non-destructive test.

All tensile testing was carried out using a Tinius-Olsen test machine and K type grips. Crosshead speed was 0.01 in./min. Specimen alignment was provided by the loading extension rods which have spherical bearing surfaces at the upper and lower heads of the testing machine. For room temperature tests, strains were measured by strain gages bonded to the front and back of the specimen to eliminate bending effects. The data reported for each test includes the following: elastic modulus, yield strength, ultimate strength, and total strain to failure. In addition, the complete stress-strain curve for each test is kept on record.

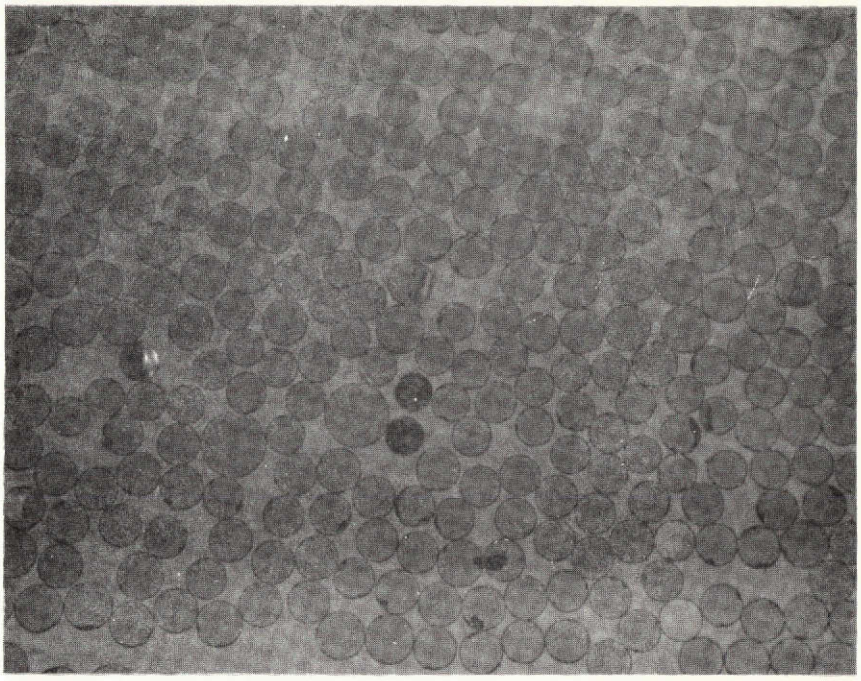

396–51 500X

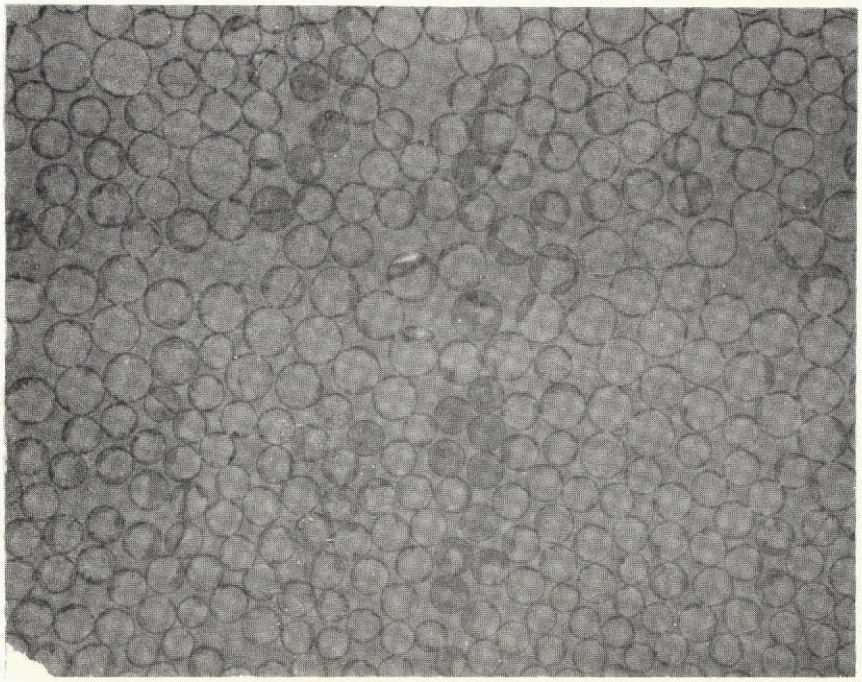

396–51 500X

This page is reproduced at the back of the report by a different reproduction method to provide better detail.

**FIGURE 1 UARL 129 FIBER GLASS–EPOXY RESIN COMPOSITES FIBER DISTRIBUTION**

Table VI

Comparison of the Tensile Properties of Several Composites

| Composite Number | Type of Fiber | Parameters of the Composite: Density gms/cm³ | Parameters of the Composite: % | Tensile Strength MN/m² | Tensile Strength (ksi) |
|---|---|---|---|---|---|
| 396-25 | UARL 129 | 2.28 | 50.2Gl, 49.8R, 0.04V | 1940 | 282.0 |
| 396-25 | UARL 129 | 2.28 | 50.2Gl, 49.8R, 0.04V | 1760 | 256.0 |
| 396-51 | UARL 129 | 2.60 | 67.5Gl, 32.8R, neg. V | 1940 | 281.0 |
| 396-51 | UARL 129 | 2.60 | 67.5Gl, 32.8R, neg. V | 1900 | 276.0 |
| 396-51 | UARL 129 | 2.60 | 67.5Gl, 32.8R, neg. V | 1900 | 275.0 |
| 396-52 | UARL 129 | 2.38 | 56.7Gl, 43.8R, neg. V | 2190 | 318.0 |
| 396-52 | UARL 129 | 2.38 | 56.7Gl, 43.8R, neg. V | 2000 | 290.0 |
| 396-56 | UARL "S" | 2.04 | 62.0Gl, 40.0R, neg. V | 1730 | 251.3 |
| 396-57 | UARL "S" | 2.02 | 61.0Gl, 40.6R, neg. V | 1160 | 268.8 |
| 396-57 | UARL "S" | 2.02 | 61.0Gl, 40.6R, neg. V | 1880 | 272.0 |
| 396-64 | Thornel 75S | 1.56 | 53.5Gr, 47.1R, 0 V | 684 | 99.2* |
| 396-65 | Thornel 75S | 1.61 | 63.7Gr, 36.3R, 0 V | 1200 | 174.3 |
| 396-65 | Thornel 75S | 1.61 | 63.7Gr, 36.3R, 0 V | 1160 | 168.4 |
| 396-69A | Thornel 75S, UARL 129 | 2.12 | 27.8Gr, 34.2Gl, 40.7R, neg. V | 820 | 119.0* |
| 396-69B | Thornel 75S, UARL 129 | 2.12 | 27.8Gr, 34.2Gl, 40.7R, neg. V | 696 | 101.0* |
| 396-70 | Thornel 75S, UARL 129 | 2.11 | 33.0Gr, 32.4Gl, 37.4R, neg. V | 945 | 137.0* |
| 396-75A | UARL 129, Thornel 75S | 2.14 | 37.6Gl, 26.5Gr, 35.9R, 0.16V | 1010 | 146.7 |
| 396-75B | UARL 129, Thornel 75S | 2.14 | 37.6Gl, 26.5Gr, 35.9R, 0.16V | 886 | 128.5 |
| 396-76 | UARL 129, Thornel 75S | 2.10 | 34.6Gl, 30.6Gr, 34.0R, 0.746V | 966 | 140.1 |
| 695 | UARL 344 | 2.49 | 60.0Gl, 37.5R, 2.5V | 1720 | 250.0 |
| | UARL 417 | 2.55 | 71.5Gl, 37.5R, 1.0V | 2050 | 298.0 |

Gl = glass, Gr = graphite, R = resin, V = voids  *delaminated & broke under doubler, result dubious

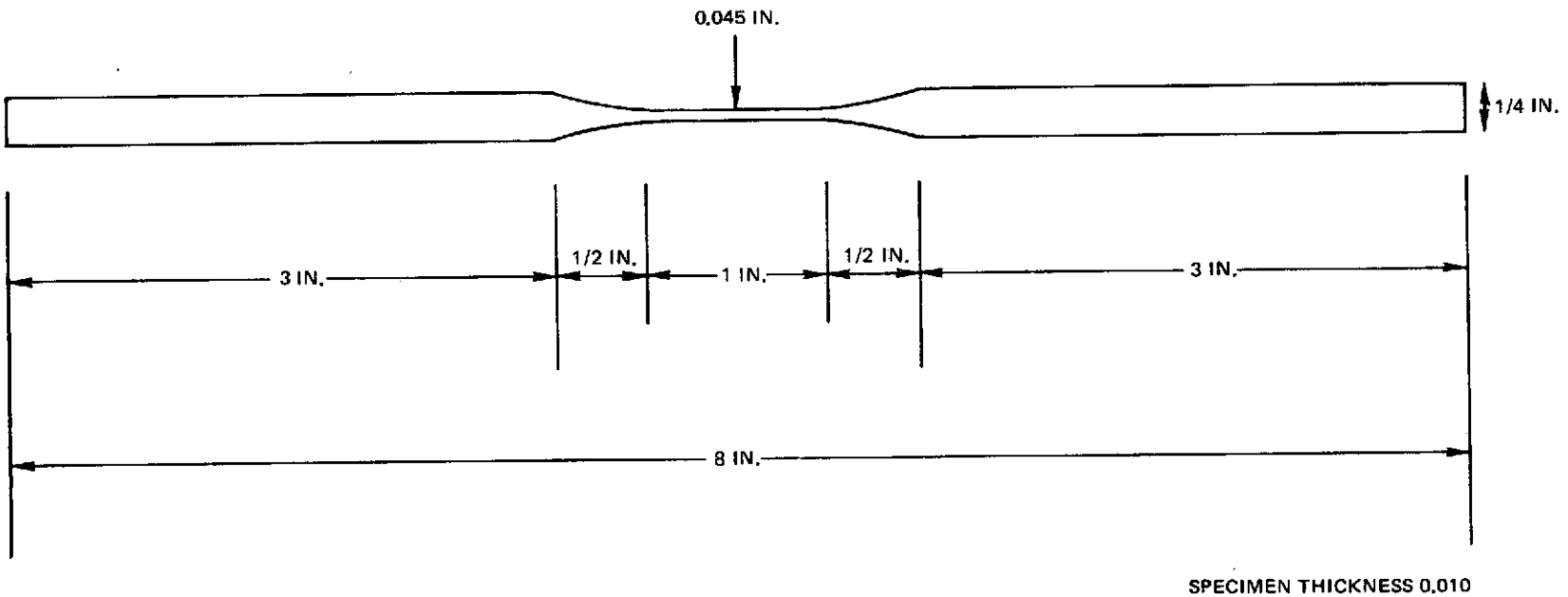


FIGURE 2. TENSILE SPECIMENS FOR UNIDIRECTIONAL GLASS FILAMENT REINFORCED COMPOSITES

## Short Beam Shear Strength of Composites

The composite shear strength is measured by use of a horizontal short beam shear test at a span-to-depth ratio of 5:1. Support pins have a radius of 3/32 in. and the loading nose has a radius of 1/8 in. The jig arrangement for measuring short beam shear strength of resin matrix composites is shown in Fig. 3. It is inserted in a Tinius-Olsen four screw universal testing machine with twelve different loading scales from 15 to 60,000 pounds full scale. All scales are interchangeable even during testing. Sample deformations can be determined either from crosshead travel or from extensometers attached directly to the specimens and this latter method is usually used. The output of the strain measuring devices can be directly recorded on an X-Y strip chart which simultaneously records the stress. A program controller allows work at constant or at cyclic stress or strain. In the glass fiber-epoxy resin test data reported in Table VII a constant crosshead speed of 0.05 in./min is used.

## Compressive Strength of Fiber-Epoxy Resin Composites

Initially, UARL tried to evaluate the compressive strength of UARL 417 glass fiber-epoxy resin composites by using the currently accepted ASTM procedure (Ref. 4) for short cylinders whose length was equal to 3 times the diameter and loading these cylinders with spherically-seated bearing blocks in the usual Tinius-Olsen testing machine. This naive approach resulted in too low a value for compressive strength as shown in Table VII and in the mushroomed samples pictured in Fig. 4.

Fortunately, the Celanese Corporation had already fully forced the problem of testing filament reinforced composites (Ref. 6). To at least partially eliminate the problem, they designed a compression jig which allows the compressive forces to be induced by shear stresses on bonded tabs in a collet type grip which does not come in contact with the test specimen. The special design specimen used is shown in Fig. 5 and the Celanese design compression test jig is shown in Fig. 6. Using this equipment we were able to completely eliminate any mushrooming effect and instead obtained gage-length failures which appear reasonable. As shown in Table VII the average compressive strength found for UARL 417 glass fiber-epoxy resin composite using the Celanese test procedure is 220,000. In our opinion this still represents a lower limit for this type of test and further testing may raise this value appreciably as we learn more about the preparation of composites.

## Fatigue Testing

All tests were conducted in a UARL constant deflection facility capable of loading the specimen in pure torsion, pure bending, and combined torsion and bending with or without a steady axial load. Figure 7 shows the machine in the

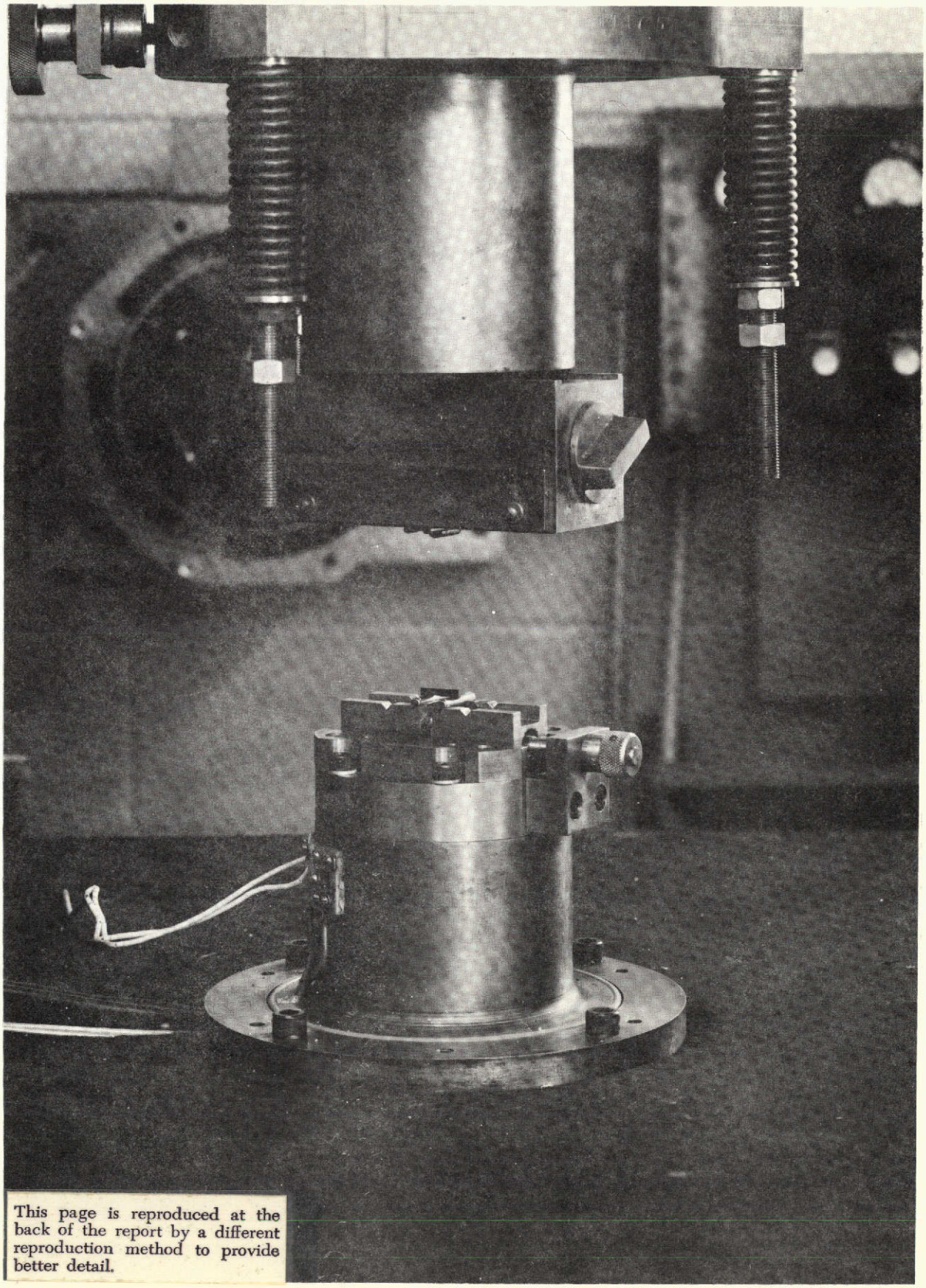

This page is reproduced at the back of the report by a different reproduction method to provide better detail.

FIGURE 3 SHORT BEAM SHEAR TEST FIXTURE

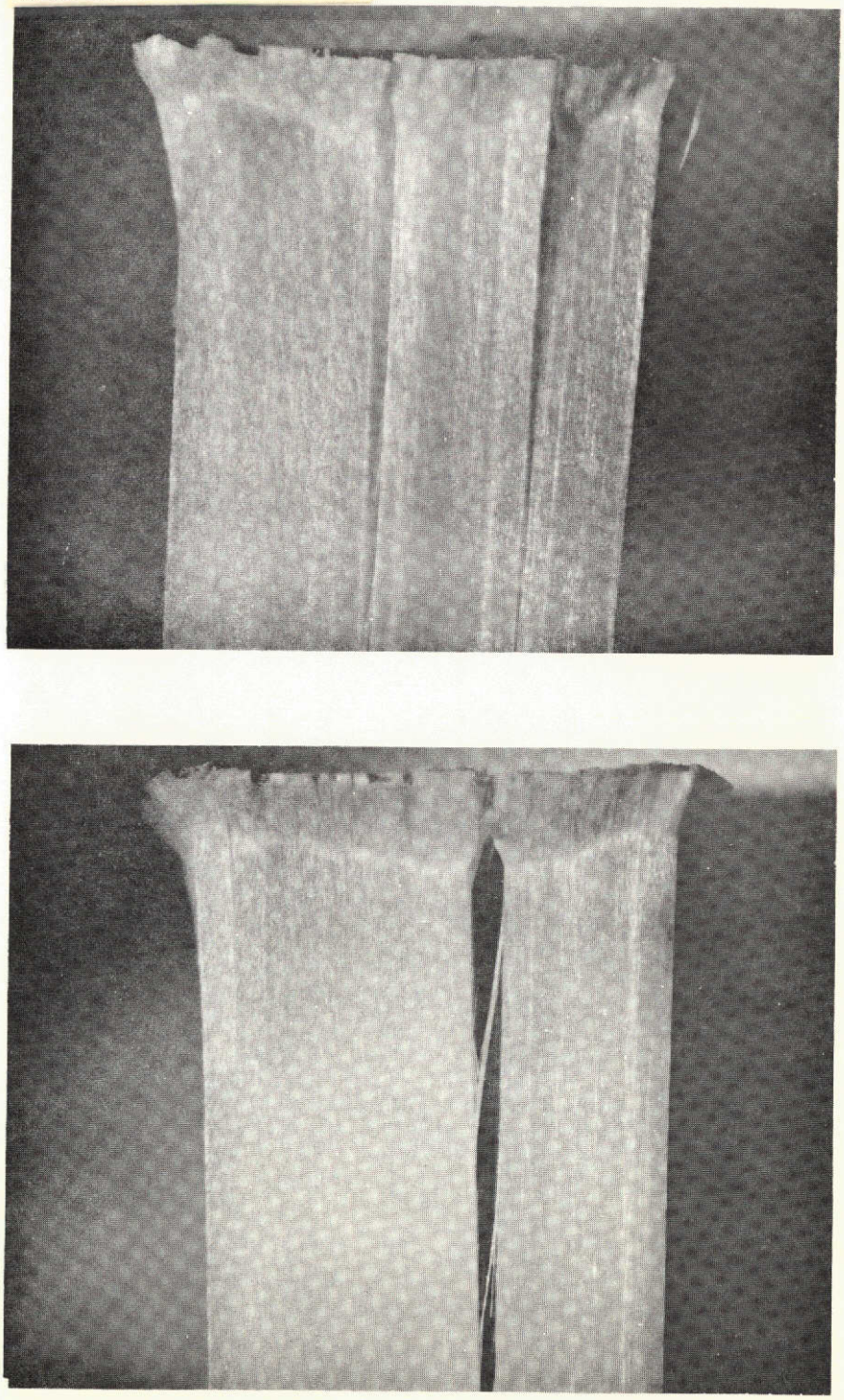

FIGURE 4 MUSHROOMING OF FIBER GLASS-EPOXY COMPOSITE IN NORMAL UARL COMPRESSION TESTING

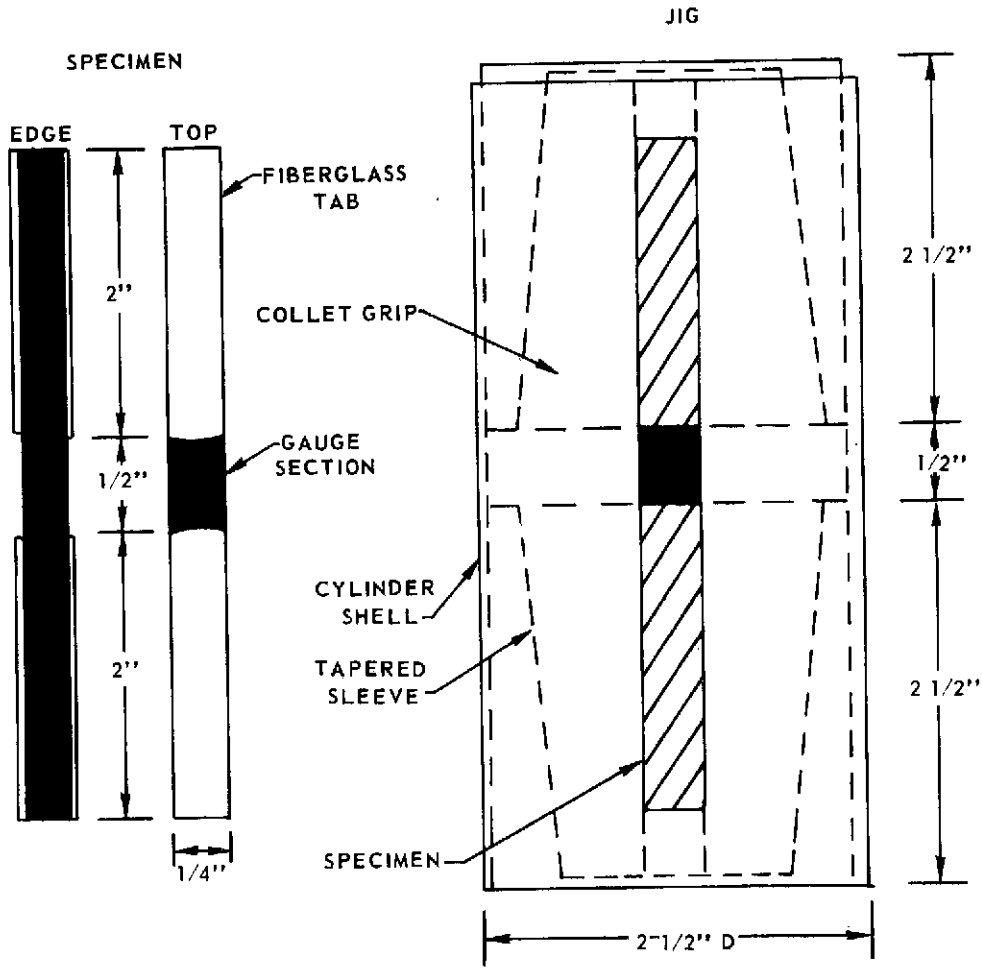


FIGURE 5. TEST SAMPLE FOR SPECIAL CELANESE CORPORATION COMPRESSION JIG

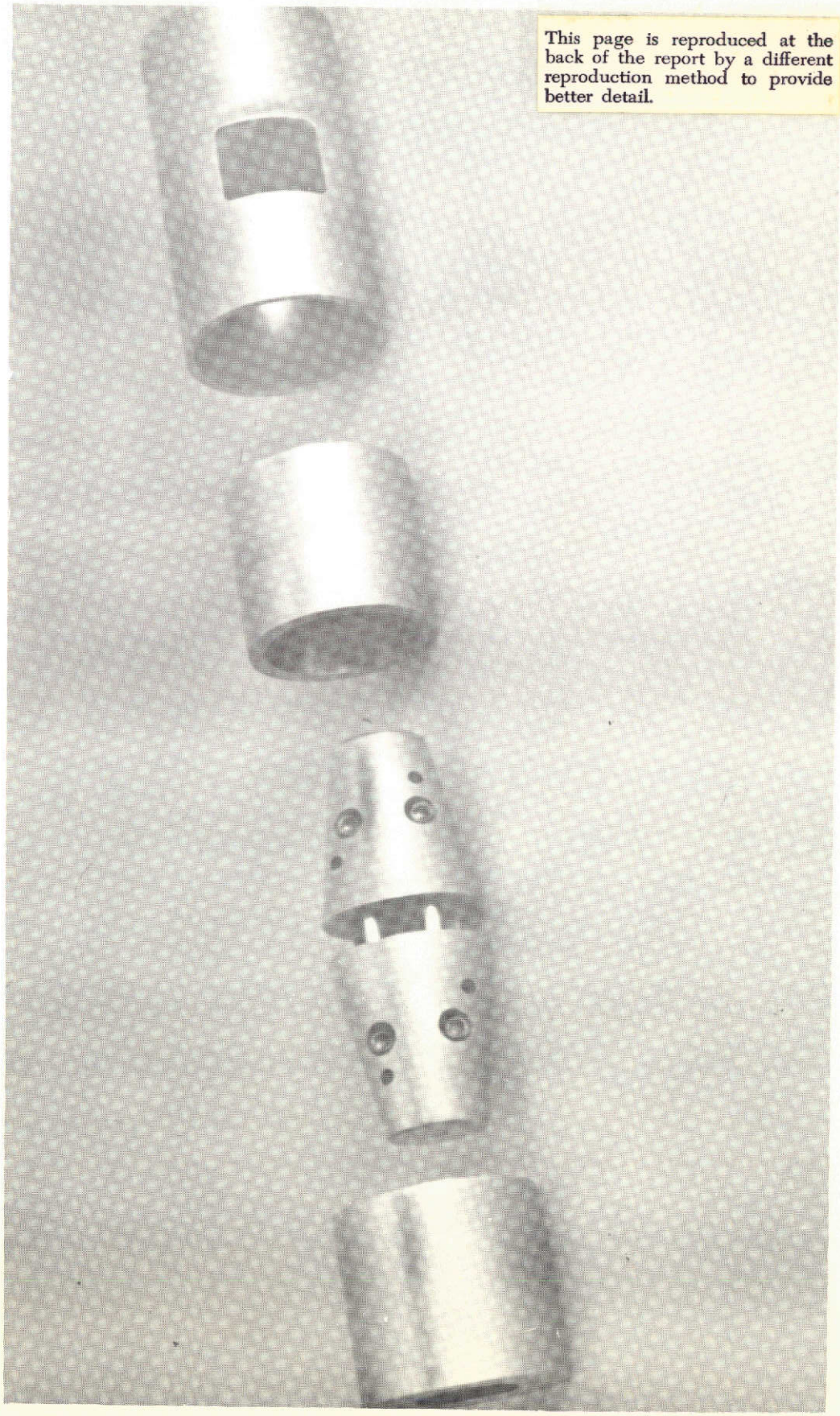

This page is reproduced at the back of the report by a different reproduction method to provide better detail.

FIGURE 6. CELANESE CORPORATION DESIGN COMPOSITE COMPRESSION RIG

Table VII

Compressive Strengths of Fiber-Epoxy Resin Composites

| Specimen Identity | Voids % | Fiber Volume % | Fiber Modulus $MN/cm^2$ | Fiber Modulus $(10^6 psi)$ | Compressive Strength $MN/m^2$ | Compressive Strength (ksi) |
|---|---|---|---|---|---|---|
| UARL 417 fiber-epoxy (unsupported specimen) | 1.0 | 71.5 | 12.1 | 17.5 | 867-841 | 117-122 |
| UARL 417 fiber-epoxy (tabbed bar) | 1.0 | 71.5 | 12.1 | 17.5 | 1500-1570 | 218-227 |
| DuPont PRD-49-I | | 65 | 13.8 | 20.0 | 276-345 | 40-50 |

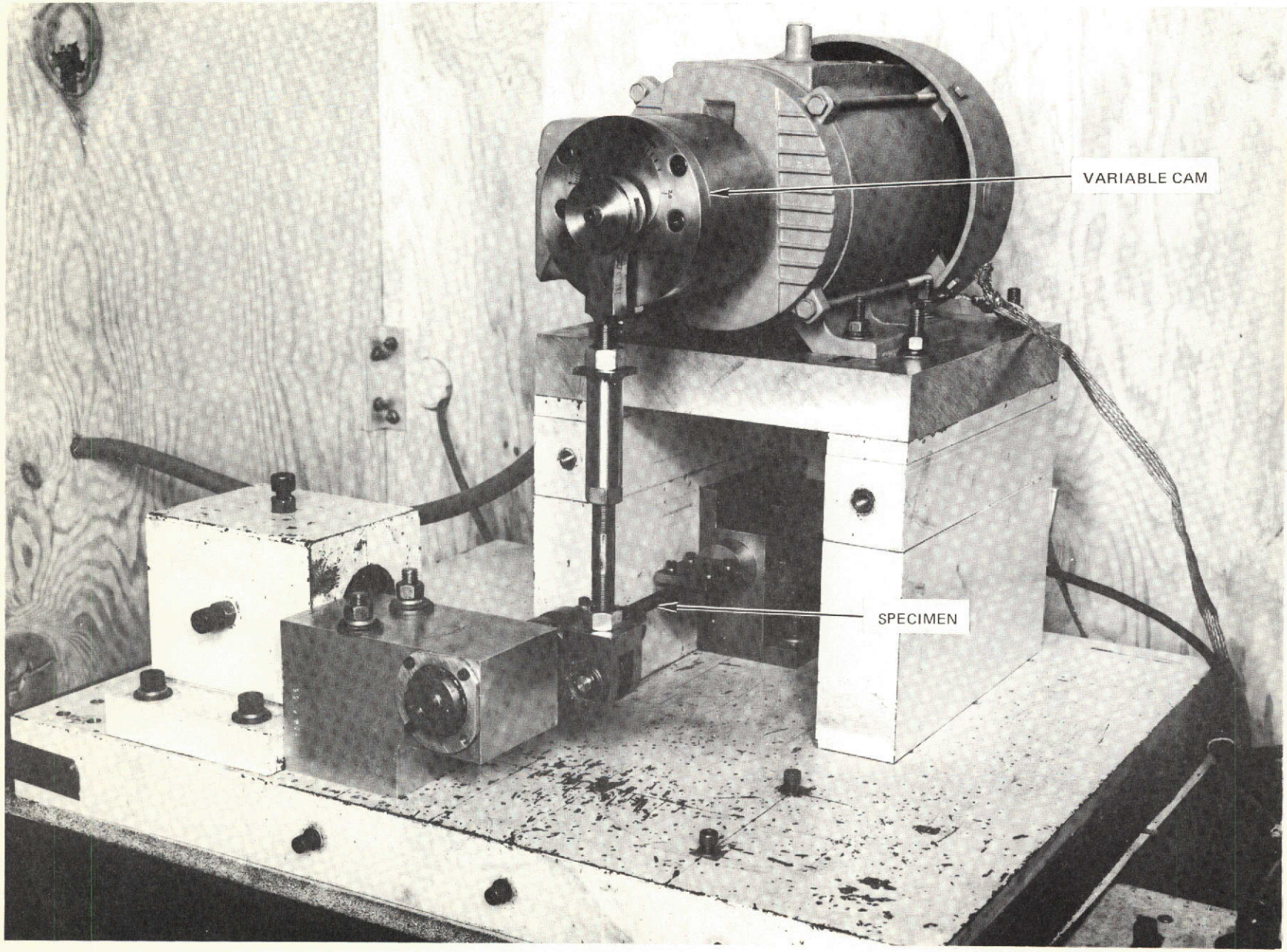


FIGURE 7. FATIGUE TEST MACHINE IN PURE TORSION CONFIGURATION

pure torsion configuration with a specimen in position for testing. Steel friction type grips are used to hold the specimen. The number of cycles accumulated during test is monitored by a timer, and the machine can be automatically stopped at any predetermined time. The speed of the motor is 3490 cpm.

In order to accurately determine the stress being applied to the test specimens, the machine was calibrated statically and dynamically using a strain gaged boron-epoxy specimen. The calibration was carried out for torsion loading only. Static calibration was accomplished by setting the variable cam at several deflections, turning the cam by hand, then reading the strain gage output with a Vishay Ellis-10 strain indicator. Dynamic calibration was obtained by displaying the strain gage output on an oscilloscope. As a result of the calibration it was concluded that the dynamic strain was 5 percent greater than the static strain for the range of deflections utilized in the program. To further insure accuracy, the static calibration was repeated each time the machine deflection was changed during the test program.

## Creep and Stress Rupture Measurements

Creep and stress-rupture measurements were made on composites in the as hot-pressed condition. The testing was performed in constant-load creep machines with automatic beam levelers. Tests were conducted at room temperature and 120°C, the temperatures being monitored by chromel-alumel thermocouples positioned adjacent to the specimen.

Specimens tested were cut from five layer composite panels. These specimens were 0.25 in. wide, 5 in. long, and approximately 0.026 in. thick, and contained approximately 50 percent filament by volume. The specimens were tested in split, friction type stainless steel grips using no reduced gage section. These grips contained replaceable insert tabs, since specimens diffusion bonded to the grips after prolonged exposures at elevated temperature under clamping pressure. The gage length was taken as the distance between the grips. One inch gage lengths were used, with 2 in. of gripping length at each end of the specimen.

It was found that the use of 0.002 in. thick aluminum doublers was necessary to insure even loading of the specimens in the grips at 300°C, however, the shear strength of the aluminum was found to be inadequate to transfer the loads at higher temperatures and 0.002 in. thick silver doublers were used at 400° and 500°C. The specimens and grips used in the creep tests were identical with those used in stress rupture tests, except that the creep tests incorporated a stainless steel extensometer attached to the grips. A photograph of the grip and extensometer setup appears in Fig. 8. Specimen elongation, actually grip

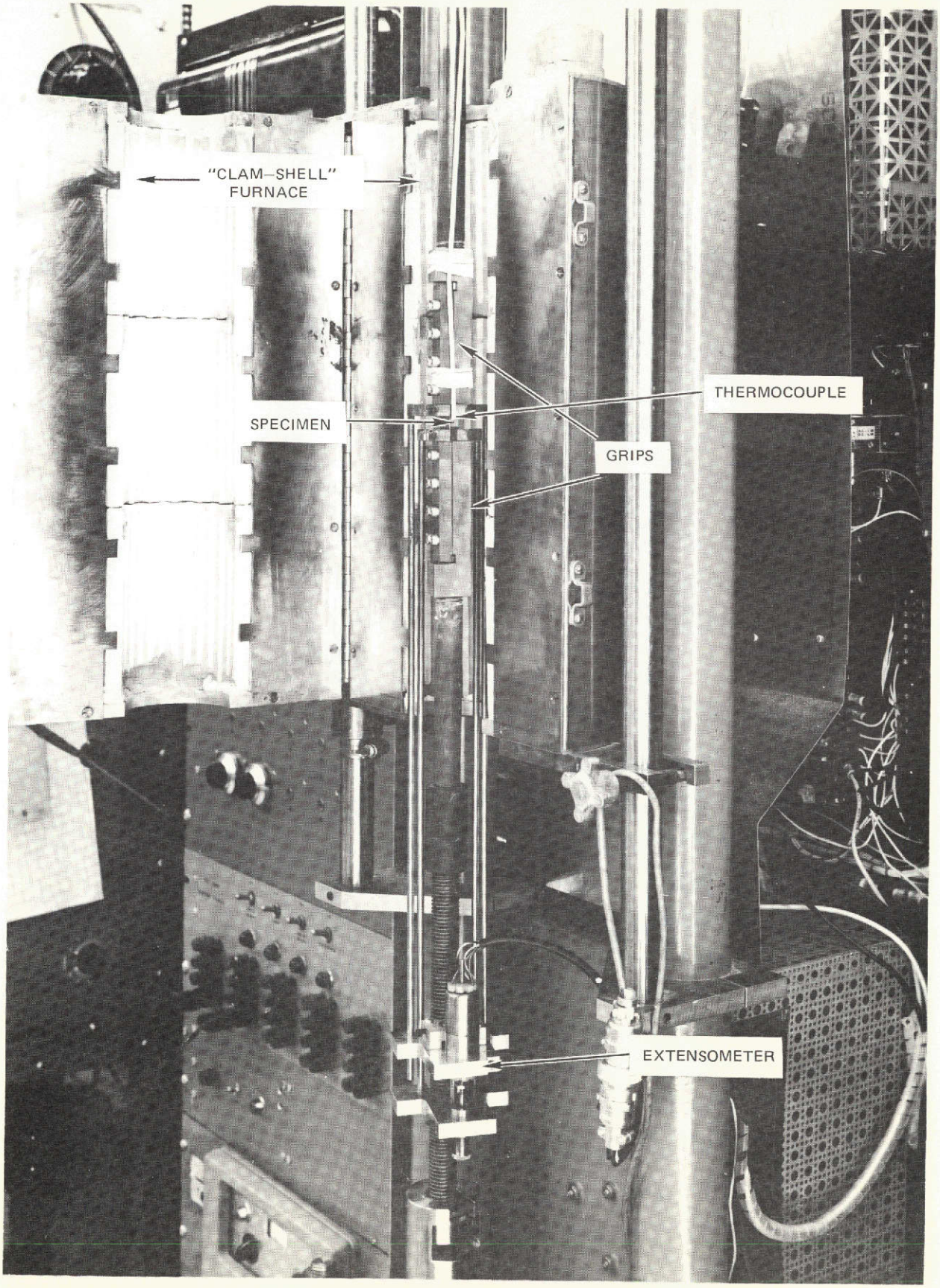


FIGURE 8. GRIPS AND EXTENSOMETER USED FOR CREEP TESTING COMPOSITES 68–104–B

N01–296–2

This page is reproduced at the back of the report by a different reproduction method to provide better detail.

movement, was continuously monitored by a linear variable differential transformer which permitted measurement of elongations as small as $1 \times 10^{-5}$ in. These experiments were also performed in the constant load creep unit with automatic beam leveler. The temperature was monitored by a chromel-alumel thermocouple and all testing was done in air.

An additional technique was used in order to differentiate between the effects of grip slippage and actual specimen elongation since the extensometers were attached to the grips rather than to the specimens themselves. The specimens were scribed with fine transverse lines which divided the gage section into eight segments. The locations of these scratches were measured by locating them under the cross hairs of a 10X microscope using a horizontally mounted depth micrometer to measure translational movement. The accuracy of measurement was $\pm$0.0005 in. The positions of the scribe marks were measured both before and after creep testing and the elongations were compared to those measured with the extensometer.

## EXAMINATION OF THE TEST DATA AND THEIR SIGNIFICANCE

Tables VII, VIII, and IX and Figs. 9 through 15 summarize the results of the physical tests made on the glass fiber-epoxy resin composites, and in several cases also show the appearance of the specimen after test. These results are discussed in individual sections for each of the testing techniques employed.

### Determination of Tensile Strength

All of the tensile strength measurements made on the five types of composites are shown in Table VII. In general, the tests are reproducible within ± 10 percent except for the data for UARL 129. If for the UARL 129 glass fiber-epoxy resin composites the results are averaged graphically by plotting the tensile strength achieved against the percent of glass fiber in the composite, the average is 283,000 psi for a glass content of 62.5 percent. The same type plot also shows that elimination of the highest and lowest results changes the average only to 282,000 psi for 61.5 percent and further that highest strength is achieved for a glass fiber content of 55 percent and the strength decreases as the glass content is raised to 67.5 percent, presumably because the increase in fiber density has caused abrasion to some inadequately protected fibers. On the same graphical basis, the average for the UARL "S" glass fiber-epoxy resin composites is 263,000 psi for 61.5 percent fiber content. The ultra-reduced cross-sectional area of the specimen as shown in Fig. 2 is probably responsible for the large scatter in the test results for the UARL 129 specimens since these were machined in advance of the other specimens and may contain machining defects eliminated by practice before the specimens were made for the last 4 composites. The typical mode of failure of the glass fiber-epoxy resin composite is shown in Fig. 9.

If the results of the tensile test data for UARL 129 and UARL "S" glass fibers are normalized to 100 percent fiber content, retained fiber strengths for UARL 129 glass fibers range up to 563,000 psi and for those for the UARL "S" glass only up to 447,000 psi which again confirms the superior absolute strength of the UARL 129 glass fiber compared to the UARL "S" glass fiber but fails to support the 12 percent increase in relative specific strength for UARL glass fiber determined on the individual fiber strength measurements. It would be apparent, therefore, that UARL has not achieved a sufficiently protective sizing for this new glass composition and that additional research in this area is necessary.

Table VIII

Comparison of the Short Beam Shear Strengths of Several Composites

| Composite Number | Type of Fiber | Parameters of the Composite: Density gms/cm$^3$ | Parameters of the Composite: % | Short Beam Shear Strength: MN/m$^2$ | Short Beam Shear Strength: (ksi) |
|---|---|---|---|---|---|
| 396-53 | UARL 129 | 2.53 | 63.4Gl, 33.7R, 2.9V | 83.4 | 12.1 |
| 396-53 | UARL 129 | 2.53 | 63.4Gl, 33.7R, 2.9V | 87.9 | 12.8 |
| 396-53 | UARL 129 | 2.53 | 63.4Gl, 33.7R, 2.9V | 84.9 | 12.3 |
| 396-54 | UARL 129 | 2.39 | 56.6Gl, 41.4R, 2.0V | 86.0 | 12.5 |
| 396-54 | UARL 129 | 2.39 | 56.6Gl, 41.4R, 2.0V | 84.1 | 12.2 |
| 396-54 | UARL 129 | 2.39 | 56.6Gl, 41.4R, 2.0V | 83.8 | 12.2 |
| 396-58 | UARL "S" | 1.99 | 59.2Gl, 41.5R, neg. V | 92.6 | 13.4 |
| 396-58 | UARL "S" | 1.99 | 59.2Gl, 41.5R, neg. V | 90.5 | 13.1 |
| 396-59 | UARL "S" | 2.08 | 67.0Gl, 34.2R, neg. V | 97.2 | 14.1 |
| 396-66 | Thornel 75 | 1.56 | 56.2Gl, 43.5R, 0.3V | 46.0 | 6.7 |
| 396-66 | Thornel 75 | 1.56 | 56.2Gl, 43.5R, 0.3V | 50.8 | 7.4 |
| 396-67 | Thornel 75 | 1.56 | 54.2Gl, 44.5R, 1.35V | 51.4 | 7.5 |
| 396-72 | Thornel 75S, UARL 129 | 2.00 | 29.9Gr, 29.6Gl, 40.3R | 68.0 | 9.9 |
| 396-73 | Thornel 75S, UARL 129 | 2.05 | 32.6Gr, 30.9Gl, 37.0R | 62.4 | 9.1 |
| 396-74 | Thornel 75S, UARL 129 | 1.96 | 26.6Gr, 26.5Gl, 49.9R | 64.1 | 9.3 |
| 396-77 | UARL 129, Thornel 75S | 2.13 | 37.6Gl, 25.5Gr, 36.4R | 48.7 | 7.1 |
| 396-78 | UARL 129, Thornel 75S | 2.02 | 33.0Gl, 27.7Gr, 35.9 | 53.4 | 7.8 |
| 396-80 | UARL 129, Thornel 75S | 2.19 | 40.9Gl, 25.5Gr, 32.1 | 57.0 | 8.3 |
| 695 | UARL 344 | 2.49 | 60Gl, 37.5R, 2.5V | 115.0 | 16.7 |
| | UARL 417 | 2.55 | 71.5Gl, 37.5R, 1.0V | 107.0 | 15.5 |

Gl = glass, Gr = graphite (Thornel 75S), R = resin, V = voids

Table IX

Comparison of Strength in Compression for Several Composites

| Composite Number | Type of Fiber | Parameters of the Composite: Density gms/cm$^3$ | Parameters of the Composite: % | Compressional Strength MN/m$^2$ | Compressional Strength (ksi) |
|---|---|---|---|---|---|
| 396-55 | UARL 129 | 2.46 | 60.0Gl, 37.8R, 2.2V | 1310 | 190.0* |
| 396-55 | UARL 129 | 2.46 | 60.0Gl, 37.8R, 2.2V | 1280 | 185.0* |
| 396-55 | UARL 129 | 2.46 | 60.0Gl, 37.8R, 2.2V | 1320 | 192.0* |
| 396-60 | UARL "S" | | | >1030 | >150.0 |
| 396-60 | UARL "S" | | | 1230 | 179.0 |
| 396-60 | UARL "S" | | | >1130 | >164.0** |
| 396-68 | Thornel 75S | 1.58 | 57Gr, 44R, neg. V | 496 | 72.0 |
| 396-68 | Thornel 75S | 1.58 | 57Gr, 44R, neg. V | 478 | 69.4 |
| 396-68 | Thornel 75S | 1.58 | 57Gr, 44R, neg. V | 363 | 52.7 |
| 396-81 | UARL 129, Thornel 75S | 2.25 | 43.0Gl, 25.6Gr, 31.8R, neg. V | 387 | 56.2 |
| 396-81 | UARL 129, Thornel 75S | 2.25 | 43.0Gl, 25.6Gr, 31.8R, neg. V | 472 | 68.5 |
| 396-81 | UARL 129, Thornel 75S | 2.25 | 43.0Gl, 25.6Gr, 31.8R, neg. V | 334 | 48.4 |
| 396-82 | Thornel 75S, UARL 129 | 2.07 | 30.6Gr, 33.9Gl, 33.6R, 2.06V | 480 | 69.7 |
| 396-82 | Thornel 75S, UARL 129 | 2.07 | | 393 | 57.0 |
| 396-82 | Thornel 75S, UARL 129 | 2.07 | | 979 | 142.0 |
| | UARL 417 | 2.55 | 71.5Gl, 37.5R, 1.0V | 1560 | 227.0 |

Gl = glass, Gr = graphite (Thornel 75S), R = resin, V = voids

*Specimen did not completely fail

**Specimen cracked longitudinally and doublers came off

This page is reproduced at the back of the report by a different reproduction method to provide better detail.

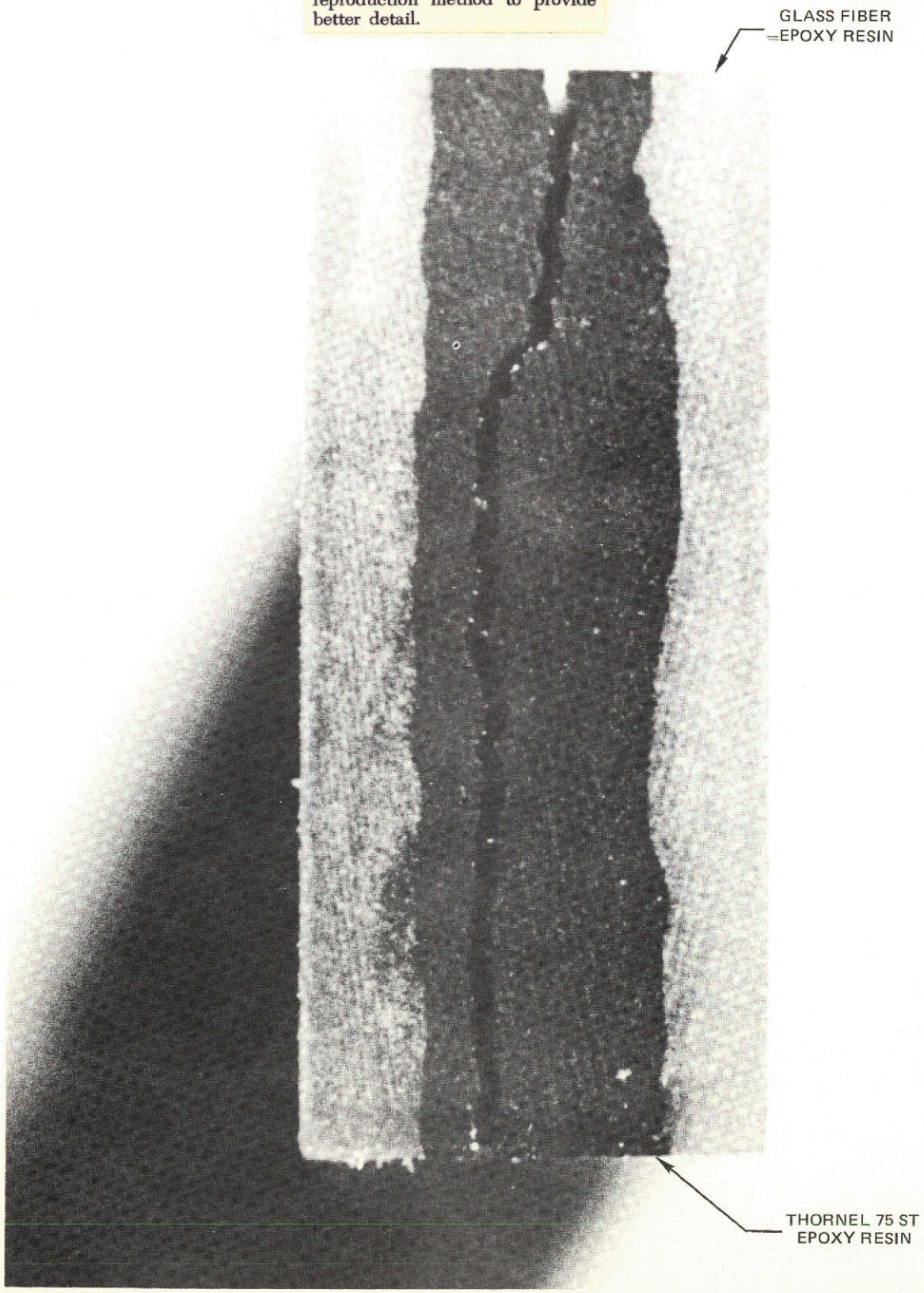


FIGURE 9. TYPICAL FAILURE MODES OF HYBRID COMPOSITES

N01–296–3

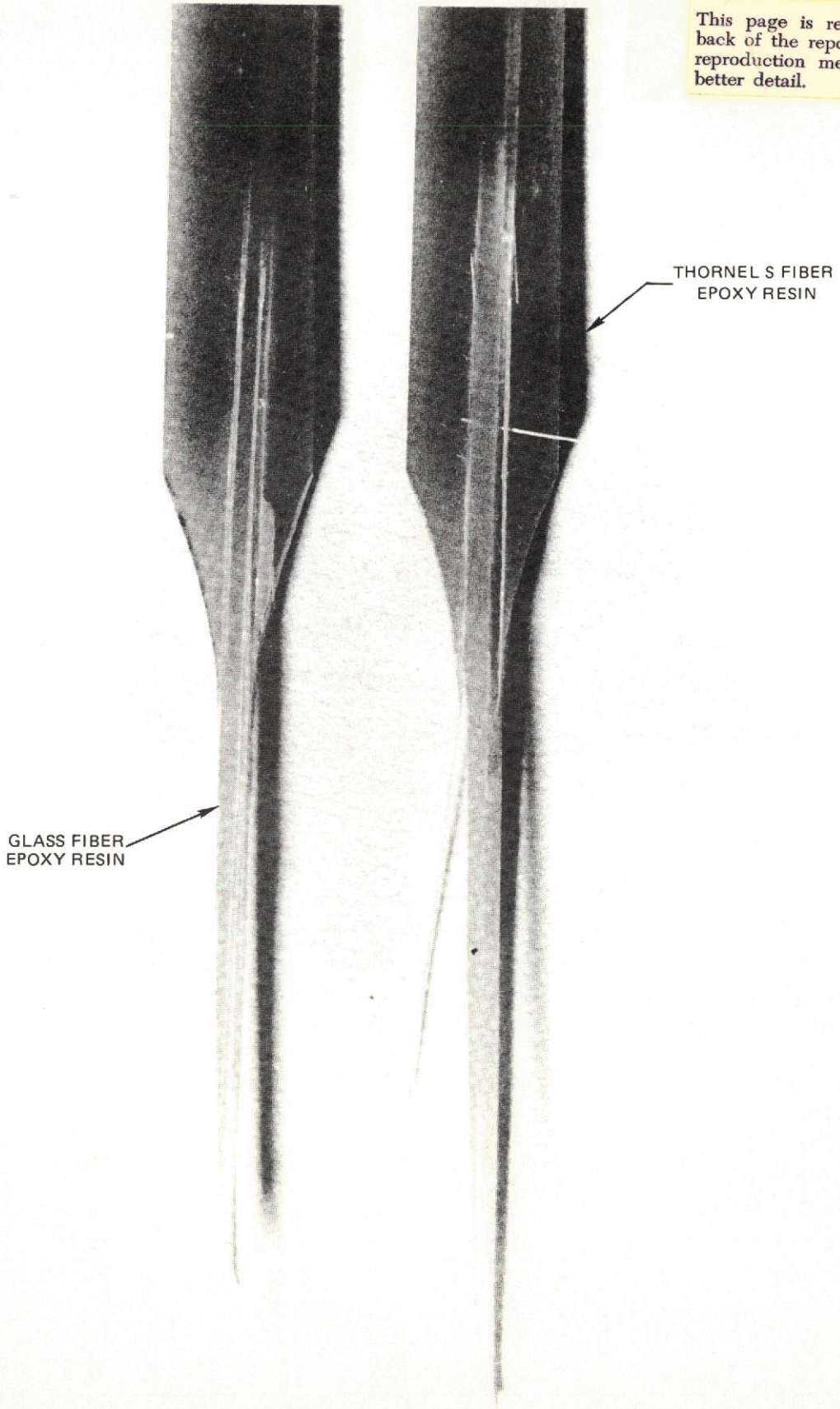


FIGURE 10. TYPICAL FAILURE OF HYBRID COMPOSITES

N01–296–4

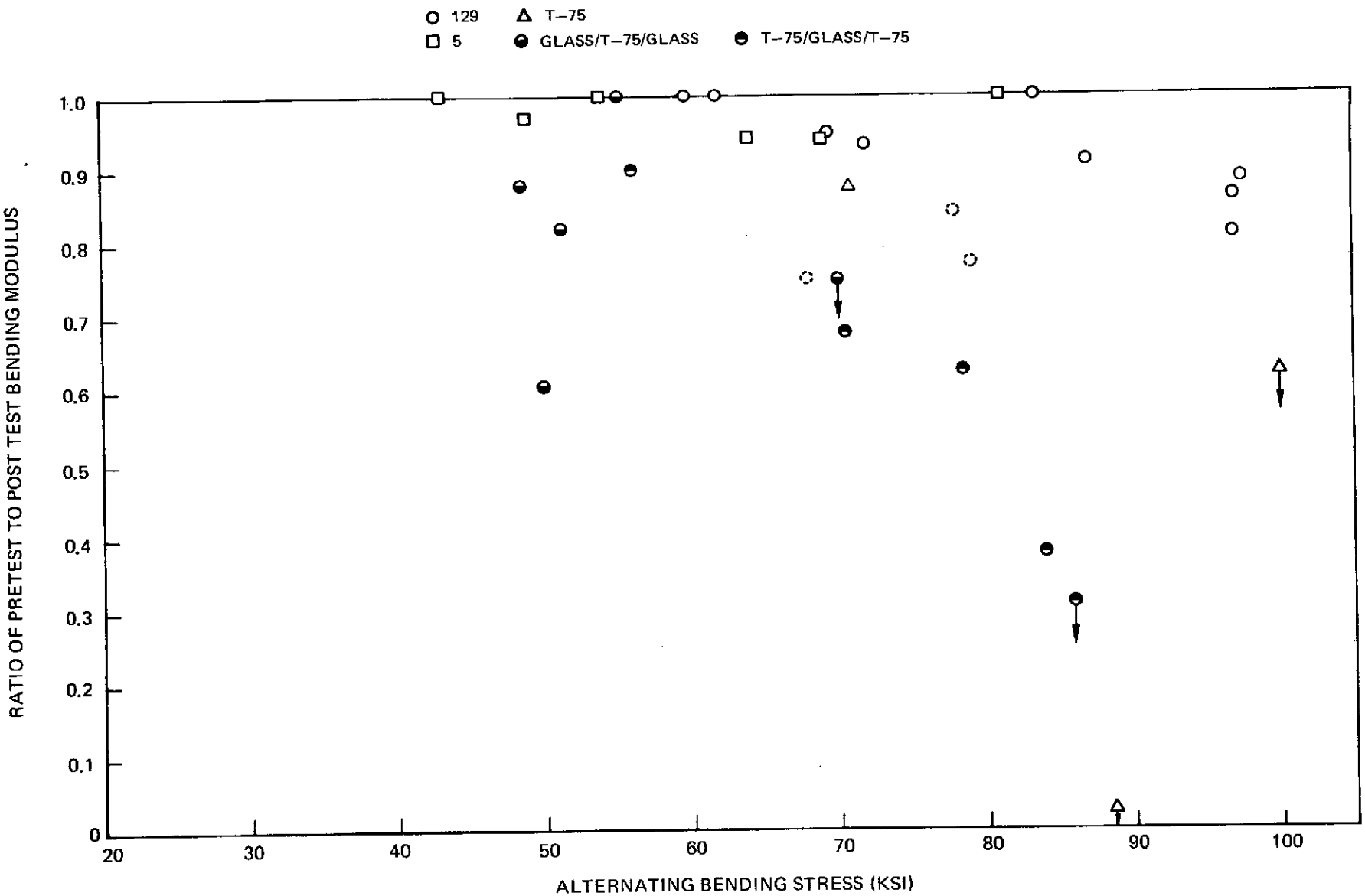


FIGURE 11. BENDING FATIGUE DATA $10^7$ CYCLES

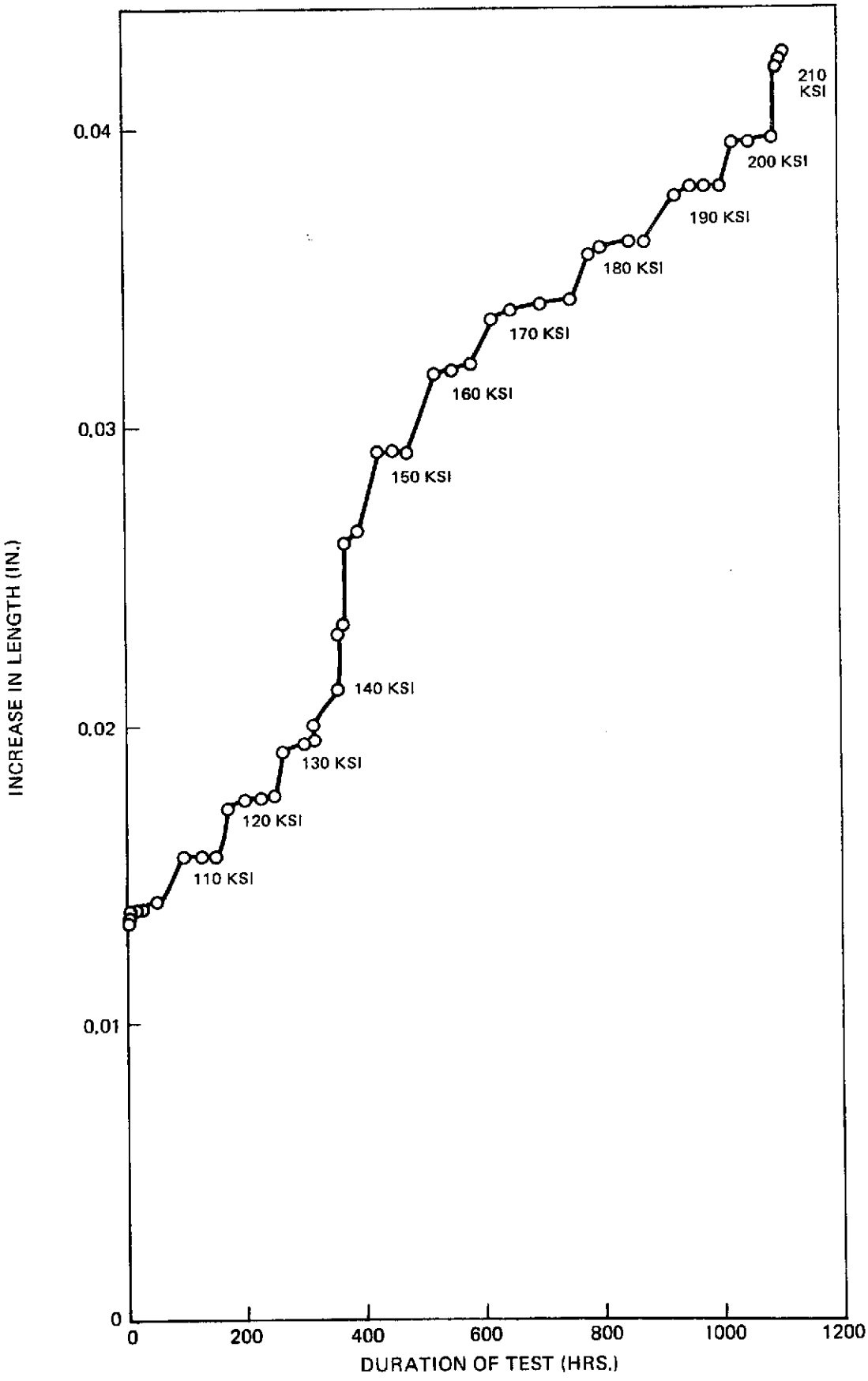


FIGURE 12. CREEP RESISTANCE AT ROOM TEMPERATURE OF UARL 129 GLASS FIBER–EPOXY RESIN COMPOSITE

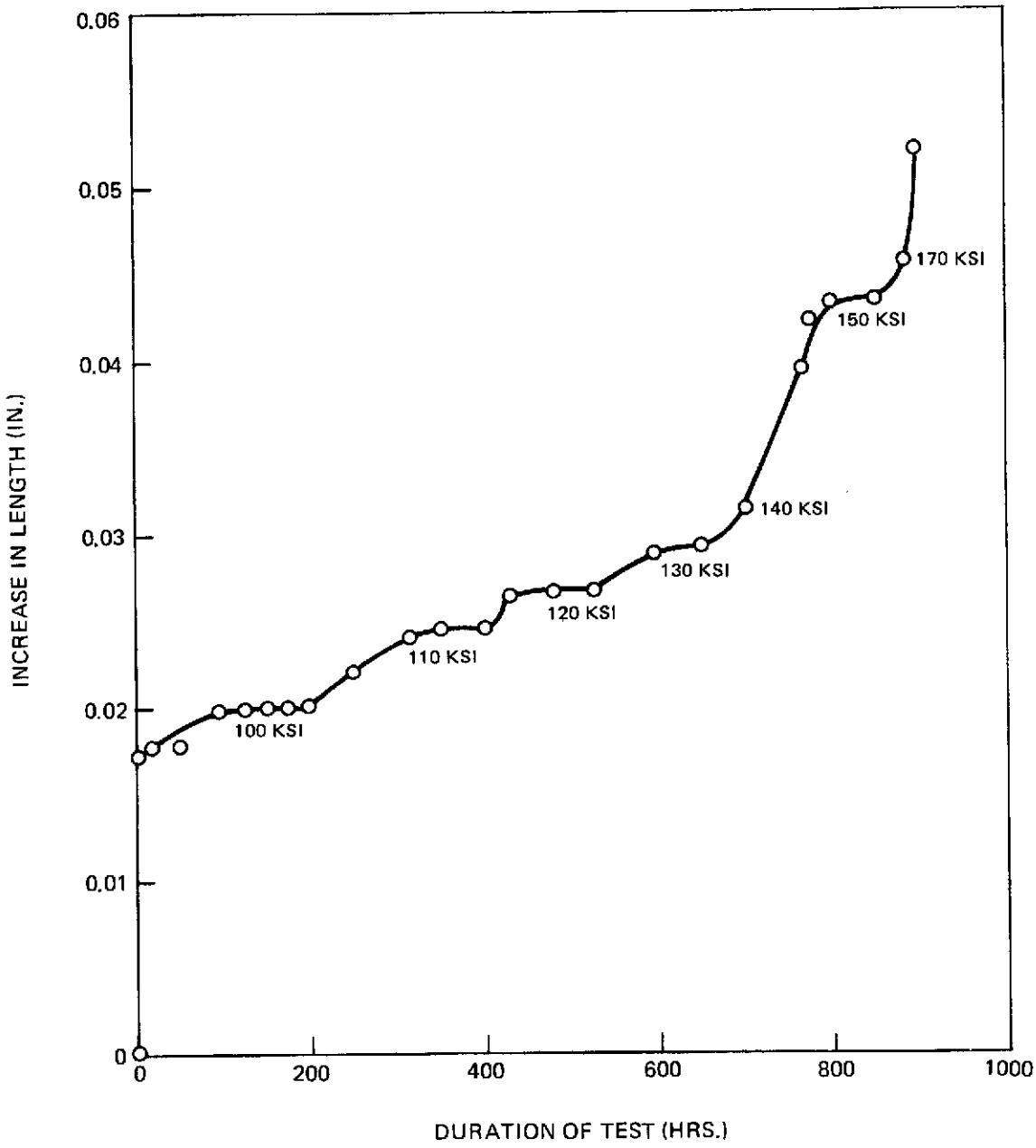


**FIGURE 13. CREEP RESISTANCE AT ROOM TEMPERATURE OF UARL "S" GLASS FIBER–EPOXY RESIN COMPOSITE**

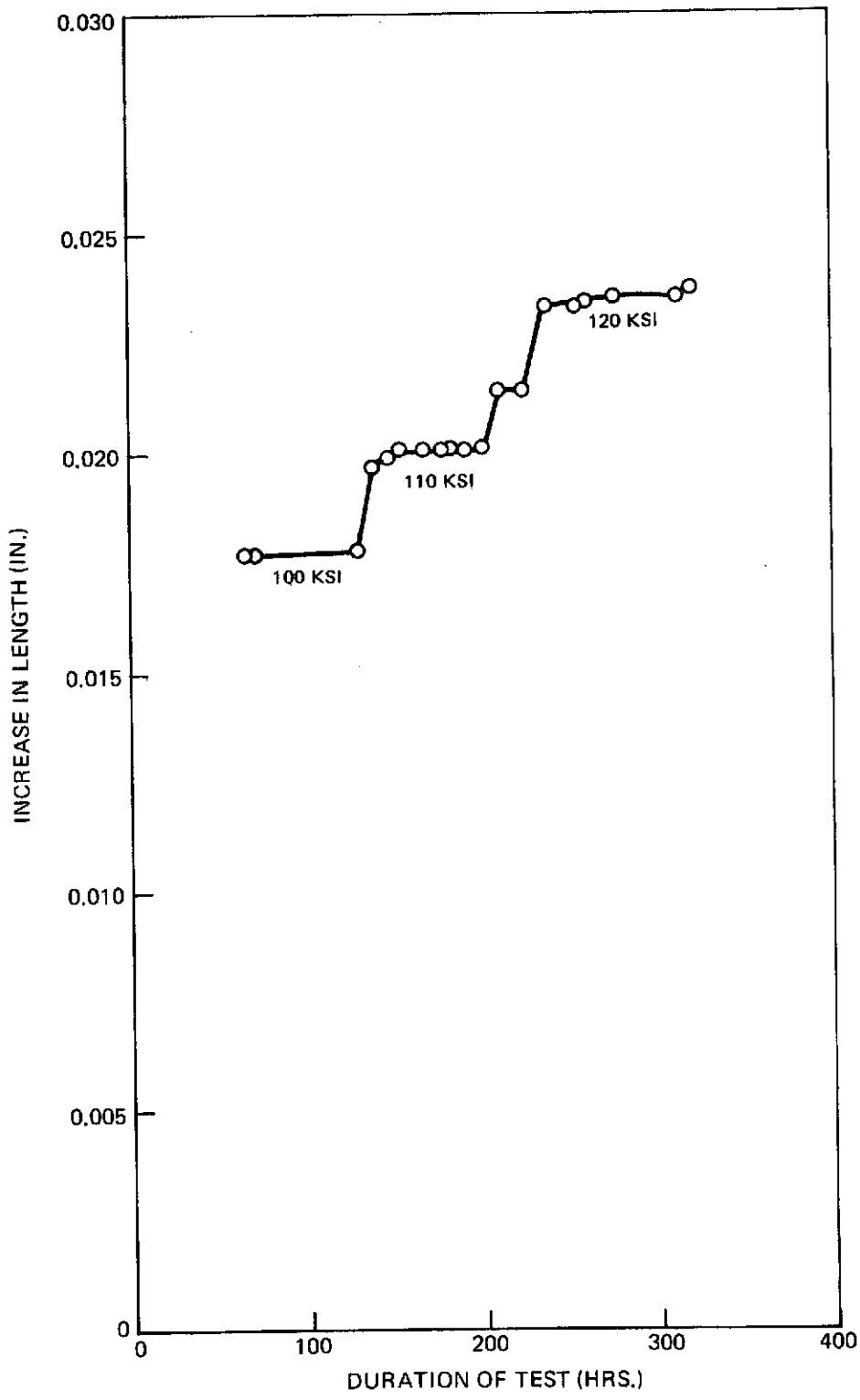


**FIGURE 14. CREEP RESISTANCE AT 100°C OF UARL 129 GLASS FIBER–EPOXY RESIN COMPOSITE**

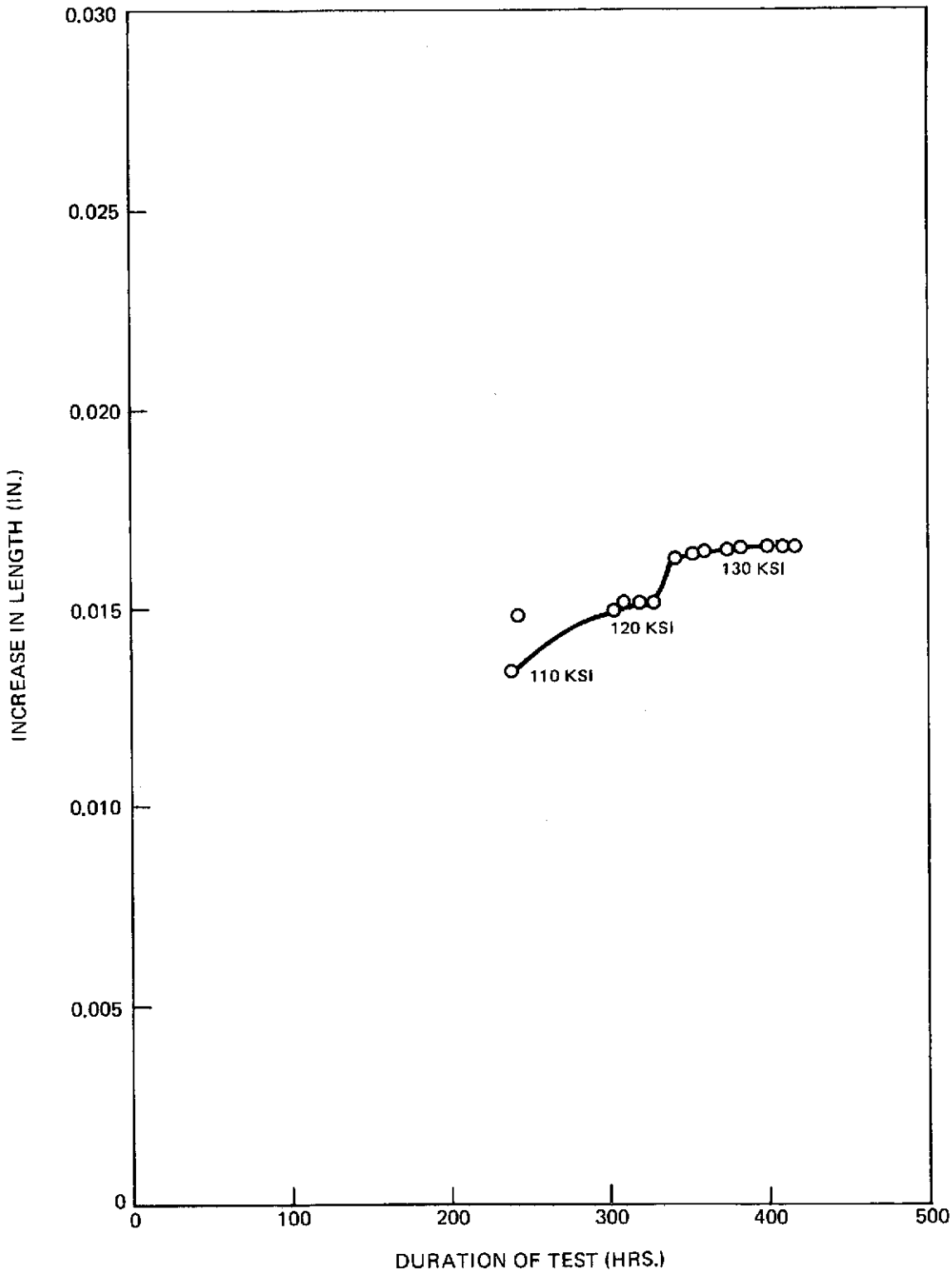


**FIGURE 15. CREEP RESISTANCE AT 120° C OF UARL 129 GLASS FIBER–EPOXY RESIN COMPOSITE**

The tensile strength data for those composites made with only Thornel 75S graphite fiber and epoxy resin is in good agreement for similar composites made in other laboratories. The tensile strength data for the hybrid composites in which Thornel 75 graphite fiber is incorporated in the outer quarters and UARL 129 glass fiber in the inner quarters is extremely doubtful since all of these hybrids delaminated and broke under the doublers. The results for the hybrid composites 396-75A and 396-76 where the outer quarters of the composite are reinforced with UARL 129 glass fiber and the inner quarters with Thornel 75S graphite fiber are believed completely valid since the breaks occurred at the correct region and have the correct appearance. Here the graphite fiber breaks first at about half the stress carried by the pure graphite composites and the load is immediately transferred to the glass fiber until they reach half the stress achieved by the pure UARL 129 glass fiber-epoxy resin composites. The results for these hybrids are, therefore, credible and show that the presence of the glass does strengthen the composite.

## Determination of Compressive Strength

The compression strength test procedure used at this laboratory has been fully described in a previous section. UARL believes that the Celanese Corporation procedure described is one of the best procedures available currently for these very strong unidirectional composites, and indeed, this test procedure consistently yields numbers higher and more in keeping with other test data than do other procedures. Nevertheless the procedure is far from perfect and all that can really be said about the test results are that these materials are at least this strong, for in many cases these compression samples split longitudinally and especially in the grip area before failing. On this basis it can be seen from the data in Table IX that the UARL 129 glass fiber-epoxy resin composites are somewhat stronger than the UARL "S" glass fiber-epoxy resin composites and that both types of glass fiber composites are more than twice as strong as the graphite fiber-epoxy resin composites. For the graphite fiber-epoxy resin composites the data appear to be the most reliable since these break at 45° to the axis to give a typical brittle material failure.

In examining the data for the hybrid composites it clearly is apparent that the UARL glass fibers placed on the two outside quarters of the hybrid sandwich help only a little after the brittle graphite central member suffers failure since the two unsupported outside quarter glass fiber composites are thin enough to fail by buckling of the unsupported columns. Here in these composites the graphite composite member again fails correctly at 45° to the axis of stress in the manner expected for brittle materials. The glass composite merely buckles, however, and does not fail by breaking. On the other hand, where the outside quarters of the hybrid composite are formed by the

brittle failure prone graphite fiber-epoxy resin composite and the inside half by the glass fiber-epoxy resin composite, the resulting hybrid composite attains a compressive strength very nearly equal to those composites formed solely from glass fiber-epoxy resin. The only valid test data here are that for composite 396-82B. The glass fiber interior of the hybrid composite consequently does a very remarkable job in strengthening this type of hybrid composite because the glass fiber-epoxy resin member is too thick now to readily buckle. For these hybrid composites the ones with the graphite member on the inside again gave a 45° to axis type of brittle failure as expected.

## The Examination of the Short-Beam Shear Strength Composite Data

In contrast to the tensile strength and compressive strength tests just discussed, the short beam shear test is dependent not only on the reinforcing fiber present in the composite but on the sizing and coupling agents used to coat the fiber since these will determine the amount of bonding present in the resultant composite. The results of the comparison of the short-beam shear strengths of the several composites shown in Table VIII are all respectable and are about what is expected. The slightly lower short-beam shear strength of the UARL 129 glass fiber reinforced composites are largely the lack of proper sizing for this glass composition as may be seen by contrast with the results of the unsized fiber composites formed with UARL 344 and 417 glass fiber reinforcements. The values for the Thornel 75S graphite fiber composites are as expected. The UARL 129 glass fiber when used to reinforce the central half of a hybrid composite with outer quarters reinforced with Thornel 75S has a decidedly beneficial result while the reverse hybrid with the outer quarters reinforced with glass fibers are not strengthened very much. That this result is as to be expected can be seen from Fig. 10 which shows a typical mode of failure for a hybrid composite in which the Thornel 75S graphite fiber is used to reinforce the central half of the composite while the glass fiber, UARL 129, is used in the outer quarters. The shear break occurs almost exactly along the central axis of maximum shear as to be expected and at a value only a little greater than that for the brittle member alone. In the hybrid composites formed in the reverse manner with the Thornel 75S graphite fiber reinforcement on the outside, the shear break occurs either in the Thornel 75S member or, in one case, along the bond between the two types of composites.

## Fatigue Test Results

Fatigue tests were conducted in a cantilever bending mode at a speed of 1800 cpm. All tests were run under constant deflection conditions. Bending stresses were calculated from the deflection, $\delta$, the specimen thickness, t, the specimen modulus, E, and the cantilever length, $\ell$, as follows:

$$\sigma = \frac{3 \delta t E}{2\ell^2}$$

The tensile modulus was determined by a rule-of-mixtures calculation.

The performance criterion was a change in composite bending modulus as a result of the test. Previous work at UARL has demonstrated that significant reductions in torsional and/or bending modulus can occur as a result of bending fatigue prior to gross fracture of the specimen. The change in bending modulus was monitored by periodically measuring the static deflection of each specimen under cantilever loading conditions.

The results of the test are presented in the accompanying figure, Fig. 11. All data points are for $10^7$ cycles with the exception of those having an arrow. Those specimens were found to suffer the indicated reduction in bending modulus at fewer than $10^7$ cycles. The 129 glass specimens showed very consistent behavior with the exception of three tests which are indicated by dotted circles. These specimens were all taken from the same composite and the fact that they were significantly different from all the others may indicate some abnormality in that composite. Due to constraints of the testing equipment it was not possible to load the S-glass composites in excess of 81 ksi. Up to that point the S-glass and the 129 glass performed in a similar manner. The Thornel 75 specimens were the only ones which showed bending failures, i.e. tensile failures in the region of the clamp. Incorporation of 129 glass on the outside produced a predominantly delamination failure, while hybrids with the 129 on the inside generally failed due to a tensile cracking of the T-75 as well as delamination.

These tests and previous tests conducted by UARL on boron- and carbon-epoxy composites indicate that delamination failures generally control the performance of these materials in bending fatigue. Based on microscopic examination of composites tested under internal programs, the weakest link under the stress state produced in this cantilever bending test is apparently the bond between the fiber and the resin. As a result of the delamination failure mode it is not surprising that the incorporation of high tensile strength glass into the Thornel 75 composites did not improve the bending

fatigue performance over that of pure T-75/epoxy, since the relatively weak bonds between the graphite and the epoxy still existed. In addition, the core-shell type of hybrids used created distinct interfaces between layers of widely different modulus. This might have produced stress concentrations which would be expected to degrade bending fatigue performance.

The use of modulus reduction as a performance criterion can be challenged as being unduly conservative since the specimens were still intact after the test. However, for several structures where composites should see application, the frequency response of the part is an important design criterion. These structures include helicopter rotor blades and gas turbine engine blades. The exact change in modulus or frequency which could be tolerated in such parts would depend on the specific application, but using information similar to that generated under this program, such a decision could be made.

## Creep Test Results

Creep tests in the sense in which the metallurgist speaks of them probably do not apply to glass fiber reinforced composites. We cannot, for example, envision rates of creation of dislocation loops or stresses required to bow dislocations past two dispersoid obstacles as in the case of metals. Here in fiber reinforced composites when the function of the matrix is to transmit load to the reinforcing glass fiber and the glass fiber is not going to show any creep, creep test data are very sensitive to grip slippage and failure, when it occurs, is probably not creep incurred but is a result of static fatigue. A thorough study of static fatigue phenomena in glass fiber reinforced plastics would involve elaborate research on the effect of a loading rate.

With these reservations, the creep test data obtained at UARL are presented in Figs. 12-15. At room temperature, UARL 129 glass fiber-epoxy resin composite failed at 210,000 psi and 1100 hrs while the UARL "S" glass fiber-epoxy resin composite failed at 170,000 psi and 900 hrs showing the marked resistance in static-fatigue resistance of UARL 129 glass fiber which would be expected because of its less moisture sensitive composition. At 100°C, the epoxy-resin loses part of its ability to transmit load to the UARL 129 fiber and failure occurred at about 300 hrs and 120,000 psi. The test at 120°C continues and the UARL 129 glass fiber composite has not yet failed at 130,000 psi and 400 hrs. The very nearly equal steps shown in Fig. 12 (except for the step between 140 ksi and 150 ksi due to sticking extensometers) show clearly that the UARL glass behaves in an elastic manner.

## RESEARCH THAT INDICATED POSSIBLE NEW DIRECTIONS FOR FUTURE RESEARCH

The present program had as one of its principal objectives the elimination of the beryllia content of the UARL 344 and 417 glasses previously developed. A strong first step in achieving a non-beryllia containing glass fiber similar to the UARL 344 and 417 fibers proved to be possible by the proper formulation of the four component non-beryllia glass system - silica, magnesia, alumina, and yttria. This formulation, UARL 129, was then used to produce the many samples specified in the research contract. Toward the end of the contract, a new composition was found, UARL 529, which had a reduced total rare-earth content (8 mol percent in place of 10) and which has half the yttria replaced by ceria so that the essential ingredients are cheaper, yet which maintains the same specific fiber modulus as UARL 129 and which still can be drawn mechanically at high rates of speed (6000 ft/min or faster). Adding two to three percent yttria to this glass will immediately improve the current best non-beryllia glass by raising the modulus a million psi.

A second composition, UARL 481, was reevaluated and found to have the same specific modulus as UARL 129 but since it has a bulk modulus nearly two million psi higher than the bulk modulus of the UARL 129 the possibility of increasing the modulus of the glass fiber by heat treatment, as it is drawn, exists. The comparative data for the three glasses UARL 129, 481, and 529 have been shown in Table VII.

A third departure from the present research which may yield a glass fiber greatly improved in strength even when compared to the strong UARL 129 non-beryllia glass fiber would rest on a recent American patent which stresses the efficiency of small but critical amounts of titania in increasing the strength of glass fibers drawn from the ternary system silica-alumina-magnesia. Adding this fifth ingredient, titania, to the very strong fibers from our quaternary system silica-alumina-magnesia-yttria should result in corresponding stress increases but would have to be studied carefully as to its effect on fiberizability, viscosity, and surface tension of the system.

A fourth direction to move in the high modulus, high strength non-beryllia glass fiber would be to increase the modulus to at least equal or surpass that of the outstanding UARL 344 beryllia glass. Recent UARL research shows that both tantalum oxide and zinc oxide additions make large contributions per mol to Young's modulus. The tantalum oxide addition is especially attractive since when added as lithium tantalate it may even result in a density decrease and subsequent increase in specific modulus for the system. An alternate approach to increasing the modulus of high-modulus, non-beryllia glasses would consist in starting with very high modulus non-fiberizable non-beryllia composition UARL 383 (Young's

modulus of 22.75 million psi compared to 16.7 million psi for UARL 129) and by measuring the effects of systematic additions on the viscosity and surface tension of this glass to arrive at a readily fiberizable extended working range high modulus non-beryllia glass.

A fifth direction that promises a large reward in increase of specific modulus by lowering the density without decreasing the modulus can be achieved by substitution of calcia for alumina and boric oxide for part of the silica as we show in a later section. Alternately, similar improvement in specific modulus is possible by the substitution of zirconia for part of the yttria. Again the addition of lithia to the composition markedly decreases the density. The extent to which such changes can be carried out without influencing the fiberizability, i.e. the relation of the viscosity to the surface tension, and still maintain a desirably high modulus and strength in the resulting glass fiber remains to be investigated.

## CONCLUSIONS

1. The evidence presented indicates clearly that a high modulus, high strength non-beryllia containing low cost glass fiber readily processable can be produced. The UARL 129 glass fiber has a modulus of 16.7 million psi, a single filament strength of 727,000 to 757,000 psi, and this fiber when incorporated in a glass fiber-epoxy resin composite shows improvement in tensile strength, compressive strength, and static fatigue resistance when compared to similar UARL "S" glass reinforced epoxy resin composites.

2. Evidence has also been presented which indicates that the UARL 129 composition can probably be readily altered to yield even higher modulus and stronger glass fibers of lower density.

3. The short-beam shear test results obtained on the UARL 129 epoxy resin composites indicate the need for research on improved sizing and coupling agents for this type of glass composition if the full potential of the glass fiber-epoxy resin composites are to be achieved.

4. Hybrid composites formed with graphite fiber reinforced epoxy resin composites on the outside quarters and glass fiber reinforced epoxy resin composites on the inside show much higher short-beam shear strengths and improved compressive strength compared to composites formed with graphite fiber alone as reinforcing agent or hybrid composites formed with graphite fiber-epoxy resin composite in the central half and glass fiber-epoxy resin composites on the outside quarters.

## REFERENCES

1. Bacon, James F.: The Kinetics of Crystallization of Molten Binary and Ternary Oxide Systems and Their Application to the Origination of High Modulus Glass Fibers, NASA Contract Report NASA CR-1856, National Aeronautics and Space Administration, Washington, D.C., Nov. 1971.

2. Bacon, James F.: Determining and Analyzing the Strength and Impact Resistance of High Modulus Glass, Final Report, Contract NASW-2209, March 15, 1972, UARL L911105-4.

3. Weyl, W. A. and E. C. Marboe: The Constitution of Glasses, Vol. II: Constitution and Properties of Some Representative Glasses, Part I. Interscience Publishers, John Wiley & Sons, New York, pp 757-790 and Sect. 5, p 531, 1964.

4. ASTM 1970 Annual Book of ASTM Standards, Part 31 (July 1970) Metals-Physical, Mechanical, Nondestructive, Corrosion Tests, Metallography, ASTM Methods E-9, E-III, AST, Philadelphia, Pa.

5. Celanese Corporation Bulletin CAC 2A-2/70 Compressive Testing for High Modulus Composites.

6. Phillips, C. J.: Calculation of Young's Modulus of Elasticity from Composition of Simple and Complex Silicate Glasses, Glass Technology, 5 [6], 216-223, Dec. 1964.

THE FOLLOWING PAGES ARE DUPLICATES OF ILLUSTRATIONS APPEARING ELSEWHERE IN THIS REPORT. THEY HAVE BEEN REPRODUCED HERE BY A DIFFERENT METHOD TO PROVIDE BETTER DETAIL